IMAGE RESTORATION TECHNIQUES FOR REMOVAL OF BLURRED IMAGES

AMEER NAEEM ZYARAH

FACULTY OF ENGINEERING
UNIVERSITY OF MALAYA
KUALA LUMPUR

2017

IMAGE RESTORATION TECHNIQUES FOR REMOVAL OF BLURRED IMAGES

AMEER NAEEM ZYARAH

RESEARCH REPORT SUBMITTED TO FACULTY OF ENGINEERING, UNIVERSITY OF MALAYA, IN PARTIAL FULFILMENT OF THE REQUIREMENTS FOR THE DEGREE OF MASTER IN ENGINEERING

FACULTY OF ENGINEERING
UNIVERSITY OF MALAYA
KUALA LUMPUR

2017

UNIVERSITY OF MALAYA

ORIGINAL LITERARY WORK DECLARATION

Name of Candidate: Ameer Naeem Zyarah

Matric No: KGE 150015

Name of Degree: Master of Engineering (Telecommunication)

Title of Research Report ("this Work"): Image restoration techniques for removal of blurred images

Field of Study: Image and signal processing

I do solemnly and sincerely declare that:

(1) I am the sole author/writer of this Work;
(2) This Work is original;
(3) Any use of any work in which copyright exists was done by way of fair dealing and for permitted purposes and any excerpt or extract from, or reference to or reproduction of any copyright work has been disclosed expressly and sufficiently and the title of the Work and its authorship have been acknowledged in this Work;
(4) I do not have any actual knowledge nor do I ought reasonably to know that the making of this work constitutes an infringement of any copyright work;
(5) I hereby assign all and every rights in the copyright to this Work to the University of Malaya ("UM"), who henceforth shall be owner of the copyright in this Work and that any reproduction or use in any form or by any means whatsoever is prohibited without the written consent of UM having been first had and obtained;
(6) I am fully aware that if in the course of making this Work I have infringed any copyright whether intentionally or otherwise, I may be subject to legal action or any other action as may be determined by UM.

Candidate's Signature Date:

Subscribed and solemnly declared before,

Witness's Signature Date:

Name:

Designation

ABSTRACT

A digital image is a two-dimensional numerical array that is produced to record a faithful yet significant scene, however more often than not the recorded image invariably represents a blurred version of the original scene. Blurring is introduced in the process of imaging due to relative motion between camera and scene, atmospheric turbulence, etc. Hence, image restoration is a fundamental research topic in the realm of image to obtain an optimal estimate of the original image given the degraded image.

This research project explores the motion blur which arises from the relative motion between camera and scene. In this study, four different techniques are used to remove the motion blur. They are Direct Inverse filter, Wiener filter, Constrained Least Squares filter, and Lucy Richardson algorithm, to restore degraded image (motion blurred image).

In this research project, an original image is motion blurred at fixed length (30 pixels) along with different angles (θ). These degraded images are then restored with the derived image restoration techniques. Statistical error image metrics (MSE and PSNR) and Human Visual System feature-based metric (SSIM) are then computed to evaluate and analyze the quality of the restored images using the aforementioned image restoration techniques. Experimental and simulation results show that Wiener filter is the best-performing image restoration technique, followed by Direct Inverse filter, Constrained Least Squares, and lastly, Lucy Richardson algorithm.

ABSTRAK

Imej digital adalah perwakilan pelbagai berangka bagi imej dua dimensi yang dihasilkan untuk merakam signifikasi imej, tetapi ianya lebih kerap daripada imej yang tidak direkodkan yang mewakili versi kabur bagi imej asal. Imej kabur diperkenalkan dalam proses pengimejan adalah kerana pergerakan relatif antara kamera dan tempat kejadian, pergolakan atmosfera, dan sebagainya. Oleh itu, pemulihan imej adalah topik penyelidikan asas dalam bidang imej untuk memperoleh anggaran optimum imej asal yang diberikan imej yang berkualiti rendah.

Projek penyelidikan ini akan mengkaji gerakan kabur yang hadir dari gerakan relative antara kamera dan imej. Dalam kajian ini, empat teknik yang berbeza diguna untuk menghilangkan gerakan kabur. Berikut adalah penapis terus songsang, penapis Wiener, penapi berkuasa rendah, dan algorithma Lucy Richardson, bagi memulihkan imej yang terdegradasi (imej kabur bergerak).

Dalam projek penyelidikan ini, imej asal yang merupakan gerakan kabur pada kepanjangan tetap (30 piksel) pada sudut yang berbeza (θ). Imej yang terdegradasi ini kemudiannya dipulihkan dengan teknik pemulihan imej yang diperolehi. Statistik ralat bagi metrik imej (MSE dan PSNR) dan sistem visual manusia (SSIM) kemudiannya dihitung untuk menilai dan menganalisis kualiti imej yang dipulihkan dengan menggunakan teknik pemulihan imej yang disebutkan diatas. Hasil eksperimen dan simulasi menunjukkan bahawa penapis Wiener adalah teknik pemulihan imej yang terbaik, diikuti oleh penapis songsang terus, penapis berkuasa rendah dan algoritma Lucy Richardson.

ACKNOWLEDGEMENTS

"In the name of Allah, the most beneficent and the most merciful"

First and foremost I would like to thank Allah Almighty subhanahu wa-ta'ala for His endless blessing and giving me the perseverance to achieve what I have achieved today.

I would like to thank and appreciate my supervisor Professor Dr. Raveendran A/I Paramesran for his continuous support, academically and personally, and great patience throughout the period it took to complete this thesis

Above all, I would like to tip my hat to my family who have given me their unequivocal support for which my mere expression of thanks does not suffice. Specifically, I am heartfully thankful to my beloved parents, eng. Naeem Zyarah and Ashwaq Abdulkareem, for their unconditional love, encouragements, guidance and support. I offer my regards and blessings to my sister for her unconditional support in all aspects during my life. Furthermore, I would like to offer my sweet love and thanks to my uncle Prof. Dr. Farid Zyarah Albehadili and all my uncles and aunts.

My special thanks to my friends Haidar, Mustafa, Ethar, Khalil, Mohamed, Dhulfiqar, Osamah, for their guidance, help and support.

TABLE OF CONTENTS

LIST OF FIGURES

LIST OF TABLES

LIST OF SYMBOLS AND ABBREVIATIONS

AD	:	Average Difference
CLS	:	Constrained Least Squares
FR	:	Full Reference
HVS	:	Human Visual System
IQA	:	Image Quality Assessment
LR	:	Lucy Richardson
MAE	:	Mean Absolute Error
MD	:	Maximum Difference
MOS	:	Mean Opinion Score
MSE	:	Mean Square Error
MSSIM	:	Mean Structural Similarity Index
NR	:	No Reference
OTF	:	Optical Transfer Function
PSD	:	Power Spectrum Density
PSF	:	Point Spread Function
PSNR	:	Peak Signal to Noise Ratio
RGB	:	Reed Green Blue
RR	:	Reduced Reference
SNR	:	Signal to Noise Ratio
SSIM	:	Structural Similarity Index

CHAPTER 1: INTRODUCTION

Image Restoration is the process of reconstructing or recovering an image that has been degraded by some degradation phenomenon. Restoration techniques are primarily modeling of the degradation and applying the inverse process in order to recover the original image. Image restoration techniques exist both in spatial and frequency domain (Xavier, 2007).

1.1 Research Background

Digital image play an important role in our daily life such as satellite television, magnetic resonance imaging, computer tomography etc. An image is a two dimensional representation of scene or object. A digital image is basically a numerical representation of an object such that digital image processing refers to the manipulation of an image by means of certain operations. An image may be defined as a two-dimensional function f(x, y), where x and y are spatial digital coordinates and amplitude off at any pair of coordinates (x, y) is called the intensity or gray level of the image at that point, where at point (x, y) the intensity value of f are finite and discrete in quantities, so we call the image a digital image. On the other hand, a color image is established by combining 2-D images individually. For instance, in the popular RGB color model, three component 2-D images, one for each primary colors, are combined to establish a color image. Hence, techniques developed for monochrome images can be applied to color images by processing the three component 2-D images separately.

An image is produced to record a faithful yet significant scene, however, more often than not the recorded image invariably represents a blurred version of the original scene. Blurring is defined as bandwidth reduction of an original image due to imperfections in the process of imaging and capturing. The introduction of blurs in recorded image includes but not limited to the following:

I. relative motion between the camera and scene

II. atmospheric turbulence

III. an optical system that is out of focus

IV. relative motion between the camera and ground

V. aberration in the optical system

VI. the short exposure time

The image degradation can be modelled as illustrate in Figure 1.1.1 and mathematically formulated as follows:

$$g(x,y) = f(x,y) * h(x,y)$$

Where $g(x,y)$ is the degraded image, $f(x,y)$ is the original image, $h(x,y)$ is the degradation function, and $*$ indicates convolution.

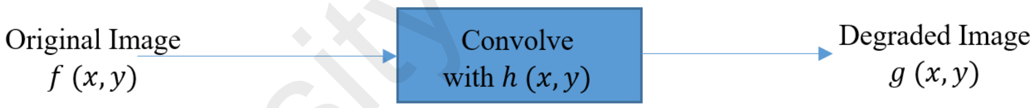

Figure 1.1.1 Image Degradation Model in Spatial Domain

Due to the fact that convolution in the spatial domain is the same as multiplication in the frequency domain, the equivalent representation of the image degradation model in the frequency domain is illustrated in Figure 1.1.2 and mathematically formulated as follows:

$$G\ (u,v) = H(u,v)F(u,v) + N(u,v)$$

Where (u,v) represents the spatial frequency coordinates whereas the terms in capital letters are the Fourier transforms of the corresponding terms in the spatial domain.

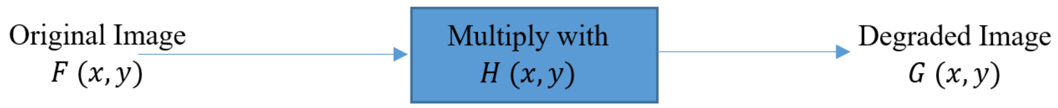

Figure 1.1.2 Image Degradation Model in Frequency Domain

Thus, image restoration, image deconvolution, or image deblurring is a fundamental research topic in the realm of image processing. Image restoration is an objective Procedure concerns with the reconstruction or recovery of an image that has been degraded. Contrary to popular belief, image restoration is distinct from image enhancement. The latter is mainly a subjective procedure comprises technique such as contrast stretching that manipulates an image to take advantage of the human visual system.

The objective of image restoration is clear-cut which is to obtain an optimal estimate $\hat{f}$(x, y) of the original image $f(x, y)$ given the degraded image $g(x, y)$, some information in regard to the degradation function $h(x, y)$.

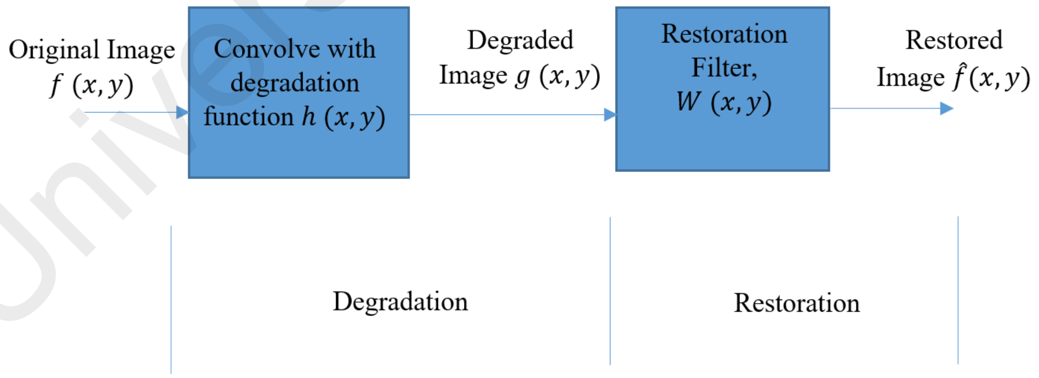

Figure 1.1.3 Image Degradation and Restoration Model in Spatial Domain.

1.2 Problem Statement

The recorded image invariably represents a blurred version of the original scene. Blurring is introduced in the process of imaging due to relative motion between camera and scene, atmospheric turbulence, an optical system that is out of focus, etc.

1.3 Objectives of Research

The main objective of this research project is to derive image restoration techniques and implement the derived image restoration techniques in MATLAB to restore a blurred image. The following outlines the detailed objectives of this research project:

I. To restore a blurred or degraded image using Direct Inverse Filter.

II. To restore a blurred or degraded image using the Wiener Filter.

III. To restore a blurred or degraded image using Constrained Least Squares (CLS) Filter.

IV. To restore a blurred or degraded image using Lucy-Richardson Algorithm.

V. To compare between Direct Inverse Filter, Wiener Filter, Constrained Least Squares Filter, and Lucy Richardson Filter

1.4 Research Report Organization

Chapter 2 discusses the related works comprehensively.

Chapter 3 outlines the research implementation as well as the image degradation model which comprises of blur model. Additionally, this chapter also discusses the image quality assessment techniques. As well as, this chapter presents the detailed derivations of each image restoration techniques employed to reconstruct the blur image.

Chapter 4 presents the restored images, computes and tabulates the image quality metrics, discusses features, challenges, as well as drawbacks of the image restoration techniques, and compares the image restoration techniques.

Chapter 5 summarizes the research with direction for future developments.

CHAPTER 2: LITERATURE REVIEW

2.1 Introduction

The goal of image restoration is to reconstruct an approximated version of the original image from a degraded observation. Image degradation occurs due to various reasons like camera mis-focus, atmospheric turbulence, camera or object motion, etc. The blurring in images due to motion is commonly encountered when there is a relative motion between the camera and object. Motion deblurring is required in many applications such as satellite imaging, medical imaging and traffic control. The motion may be linear or non-linear. The degradation due to motion can be modelled as a two dimensional linear shift invariant process. In many applications, the observed image g(x, y) can be expressed as a two-dimensional convolution of the original image with the degradation function h(x, y), and is expressed as the equation below:

$$g(x, y) = f(x, y) * h(x, y) + ŋ(x, y)$$

Where $*$ denotes the two dimensional linear convolution and (x, y) is the additive noise. The degradation function h(x, y) is also known as Point Spread Function (PSF). The degradation model can otherwise be expressed in frequency domain as,

$$g(u, v) = f(u, v)h(u, v) + n(u, v)$$

Where g (u, v), f (u, v), h (u, v), and n (u, v) are the frequency responses of the observed image, original image, PSF and noise respectively. In the absence of noise the above expression reduces to,

$$g(u, v) = f(u, v)h(u, v)$$

In classical restoration techniques, it is assumed that the PSF is known prior to restoration. So the restoration technique is just to inverse the process using frequency domain techniques with some regularization to avoid the noise amplification (Dash & Majhi, 2014).

2.2 Deblurred Motion Blurred Images

The problem of restoration of images blurred by relative motion between the camera and the object of interest. This problem is common when the imaging system is in moving vehicles or held by human hands, and in robot vision. In order to correct the image restoration, it is imperative to know the point-spread function (PSF) of the blurring system. They stated that a simplification technique for restoring motion blurred images specified only the blurred image itself. At the first, the technique determines the PSF of the blur after that applies it for restoring the blurred image. The blur identification here is based on the concept that image characteristics along the direction of motion are affected mostly by the blur and are different from the characteristics in other directions. By filtering the blurred image, and emphasize the PSF correlation properties at the expense of those of the original image (Yitzhaky, Mor, Lantzman, & Kopeika, 1998).

This study, presented a comparison of image restoration techniques, namely Wiener filter, Regularized filter and Lucy Richardson. In this research paper, an original image, see Figure 2.2.1 is motion blurred across 21 pixels at an angle of 11 degrees as presents in Figure 2.2.2 and then restored using the image restoration techniques as illustrated in Figure 2.2.3, Figure 2.2.4, and Figure 2.2.5.

Figure 2.2.1 Original Image (Yadav & Omprakash, 2013)

Figure 2.2.2 Motion Blurred Image (Yadav & Omprakash, 2013)

Figure 2.2.3 Restored Image using Lucy Richardson Algorithm (Yadav & Omprakash, 2013)

Figure 2.2.4 Restored Image using Regularized Filter (Yadav & Omprakash, 2013)

Figure 2.2.5 Restored Image using Wiener Filter (Yadav & Omprakash, 2013)

Table 2.1 PSNR of Image Restoration Techniques (Yadav & Omprakash, 2013)

Filtering Techniques	PSNR Values (dB)
Lucy- Richardson	19.83
Regularized Filter	27.28
Weiner Filter	50.93

The experimental results that is snapshots and PSNR values indicates that Weiner filter technique is the best to restore motion blurred image with an information of PSF corrupted blurred image with LEN=21 pixels and THETA=11 degrees (Yadav & Omprakash, 2013).

2.3 Image restoration Techniques

The degradation are including; blurring, quantization effects, information loss because sampling, and different sources of noise. The main purpose of image restoration is for estimating the original image from the degraded data. It is broadly applied in different fields of applications, like astronomical imaging medical imaging, photography deblurring, remote sensing, microscopy imaging, and forensic science, etc. Frequently, the benefits of enhancing image quality to the maximum possible extent for complexity of the restoration algorithms and outweigh the cost involved. In this research the comparison of different image restoration methods such as Richardson-Lucy algorithm, Wiener filter and Direct Inverse filter through PSNR (Peak Signal to Noise Ratio).

Table 2.2 Comparison of PSNR Values (dB) (Khare & Nagwanshi, 2011)

SNR	Angle	Length	Lucy	Inverse	Wiener
10	45	6	11.8423	12.8899	14.5264
30	45	6	11.8441	12.8512	14.5329
50	45	6	11.8449	12.9172	14.5339
70	45	6	11.844	12.8419	14.5343
90	45	6	11.8435	12.8899	14.5346

This experimental results showed that better restoration using Wiener filter with PSNR = 14.5346. As compare to Lucy Richardson and Inverse filter (Khare & Nagwanshi, 2011).

2.4 Image Restoration by Richardson Lucy Algorithm

This research paper, presented the performance analysis of different image restoration techniques. In this research paper, an original image is degraded through blurring and addition of a random noise. The degraded image is then restored using Inverse filter, Wiener filter, and Richardson Lucy algorithm as shown in Figure 2.4.1 and Figure 2.4.2. Restored images are then evaluated with image quality metrics, namely MSE and PSNR. Experimental results in this research paper Table 2.3 and Table 2.4 show that as the noise variance increases, the PSNR value of Inverse filter decreases. In other words, Inverse filter underperforms in the presence of noise. Furthermore, Wiener filter outperforms Inverse filter in general but loses out to Richardson Lucy algorithm. This research paper concludes that Richardson Lucy algorithm is the best-performing image restoration technique, followed by Wiener filter and Inverse filter (Thakur & Datar, 2014).

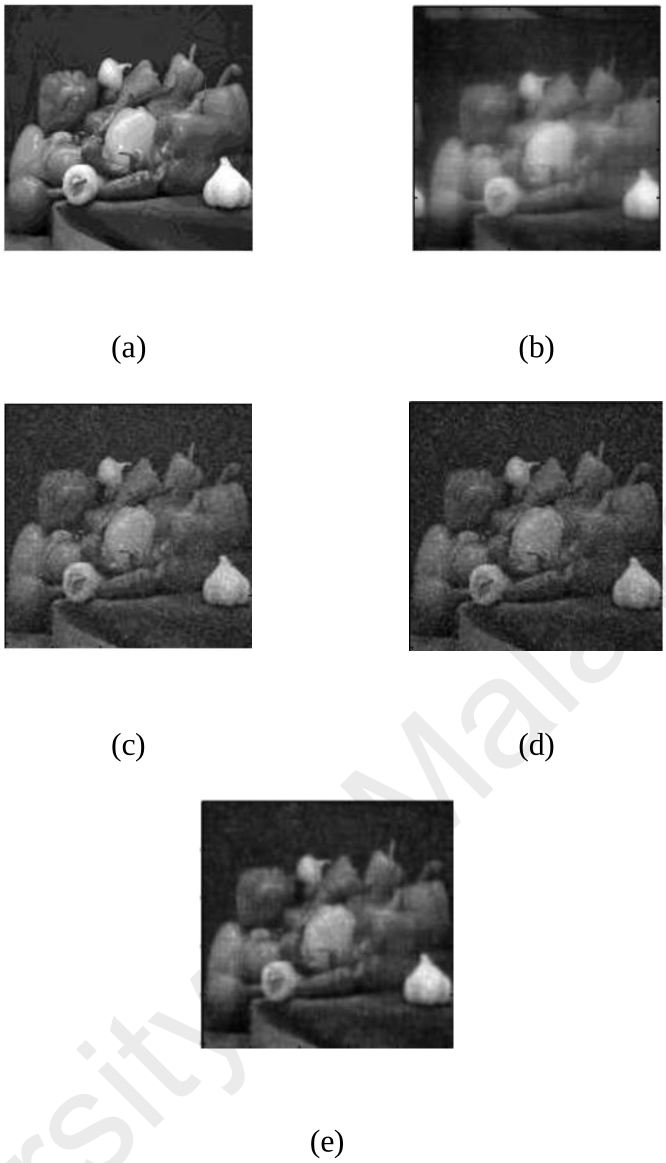

Figure 2.4.1 Results of pepper (a) original image (b) blurred image (c) Restored by Inverse filter (d) Restored by Wiener filter (e) Restored by R-L at iteration 30 (Thakur & Datar, 2014)

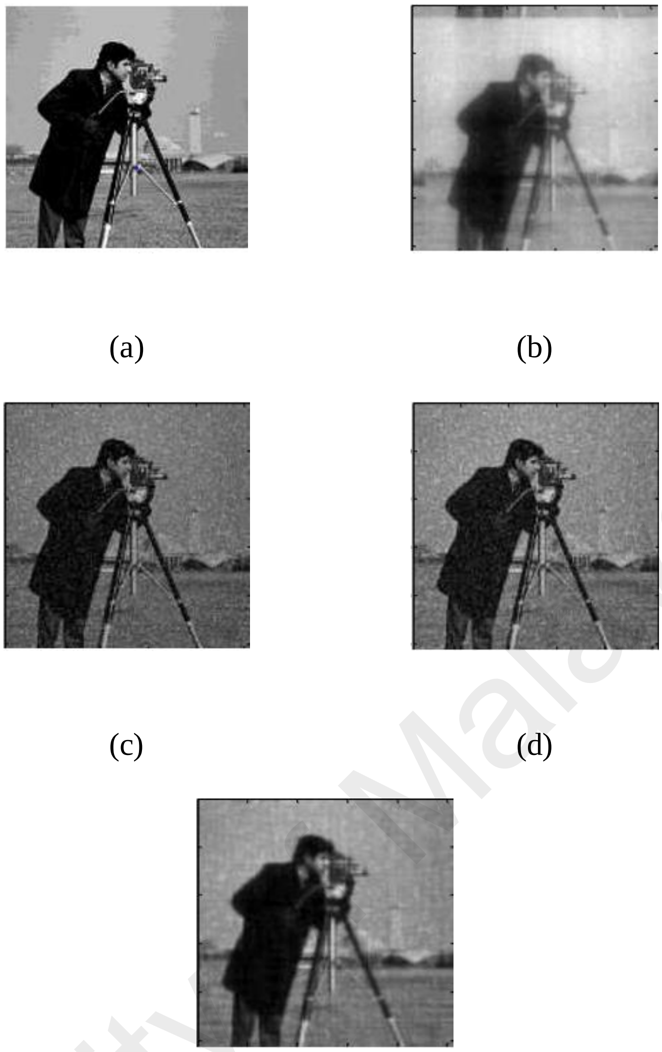

(a) (b) (c) (d) (e)

Figure 2.4.2 Results of cameraman (a) original image (b) blurred image (c) Restored by Inverse filter (d) Restored by Wiener filter (e) Restored by R-L at iteration 30 (Thakur & Datar, 2014)

Table 2.3 Results for the Cameraman image (Thakur & Datar, 2014)

Image size		256x256				512x512			
Noise variance		0.05		0.007		0.05		0.007	
		MSE	PSNR	MSE	PSNR	MSE	PSNR	MSE	PSNR
Inverse filter		0.0262	15.8123	0.0068	21.7024	0.0042	22.7645	0.0083	20.7954
Wiener filter		0.0138	18.5958	0.0061	22.1819	0.0020	27.0082	0.0028	25.5632
Richard-son lucy	Iteration 1	0.0680	11.6762	0.0654	11.8434	0.0210	16.7799	0.0440	13.5639
	Iteration 10	0.0268	15.7245	0.0245	16.1020	0.0019	27.1238	0.0064	21.9615
	Iteration 20	0.0112	19.5254	0.0071	21.5087	0.0011	29.6501	0.0022	26.6454
	Iteration 30	0.0070	21.5233	0.0035	24.6023	8.9311e-004	30.4910	0.0018	27.4981

Table 2.4 Results for the peppers image (Thakur & Datar, 2014)

Image size		256x256				512x512			
Noise variance		0.05		0.007		0.05		0.007	
		MSE	PSNR	MSE	PSNR	MSE	PSNR	MSE	PSNR
Inverse filter		0.0200	16.9817	0.0045	23.4626	0.0202	16.9483	0.0042	22.7645
Winer filter		0.0052	22.8473	0.0061	22.1819	0.0057	22.4348	0.0020	27.0082
Richard-son lucy	Iteration 1	0.0402	13.9617	0.0307	15.1323	0.0270	15.6885	0.0210	16.7799
	Iteration 10	0.0046	23.3504	0.0021	26.8659	0.0033	24.8779	0.0019	27.1238
	Iteration 20	0.0032	24.9371	0.0012	29.3916	0.0024	26.1250	0.0011	29.6501
	Iteration 30	0.0028	25.5736	9.0215e-004,	30.4472	0.0025	25.9579	8.9311e-004	30.4910

2.5 Image Restoration via wiener Filter

The performance comparison of Wiener filter between frequency domain and spatial domain. Experimental results in an ideal case where the statistical properties of original image and additive noise are known show that the Wiener filter implemented in frequency domain performs better than in spatial domain as illustrated in Figure 2.5.1 and Figure 2.5.2 (Furuya, Eda, & Shimamura, 2009).

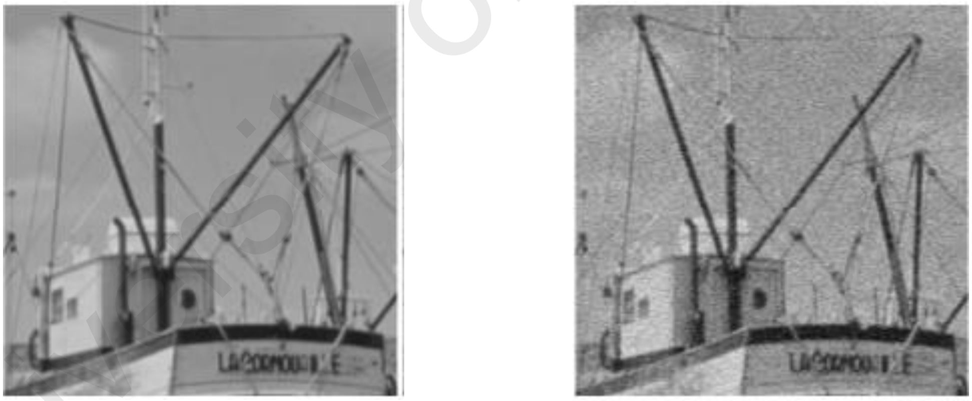

Original image

Degraded image

Figure 2.5.1 Original and Degraded image (Furuya et al., 2009)

Figure 2.5.2 Restored Images in Frequency and spatial Domain (Furuya et al., 2009)

2.6 Deblurred Image using Wiener Filter

This section, discusses on how to de-blurred image with Wiener filter with information of the Point Spread Function (PSF) corrupted blurred image with different values. Image is restored using Wiener deconvolution it works in the frequency domain, image is blurred by motion is added in image. Direct image is deblurred with using of true PSF (Point Spread Function) in Wiener Filter, if noises are not added in degraded image. Wiener filter works in the frequency domain, attempting to minimize the impact of deconvoluted noise at frequencies which have a poor signal-to-noise ratio. As shown in Figure 2.6.1 results of deblurring of images using Wiener filter. Since the PSF is varying in the motion direction, it is not correlated perpendicularly to the motion direction. If we increase length and theta of PSF, then blurring of image is increased (Mistry & Banerjee, 2014).

(a) (b) (c)

Figure 2.6.1 (a) original, (b) blurred, (c) restored image (Mistry & Banerjee, 2014)

2.7 Lagrange Multipliers in Digital Image Restoration

In this section, an image restoration technique developed based on the algorithm of Lagrange multipliers is presented. An original image is motion blurred horizontally and then restored using the proposed technique, Wiener filter, Constrained Least Squares filter, and Lucy Richardson algorithm. It is interesting to note that the simulation result as illustrated in Figure 2.7.1 shows that the Lucy Richardson algorithm requires significant computational time to accomplish the image restoration. Lagrange Multipliers is the best-performing image restoration technique.

However, proposed image restoration technique is deemed impractical because the noise is excluded in the formulation of the proposed technique. It is important to note that noise is unavoidably introduced during the image acquisition process. Hence, integration of noise into formulation or model of image restoration technique is important otherwise the image restoration technique is vulnerable to excessive noise amplification (Stojanovic, Stanimirovic, & Miladinovic, 2012).

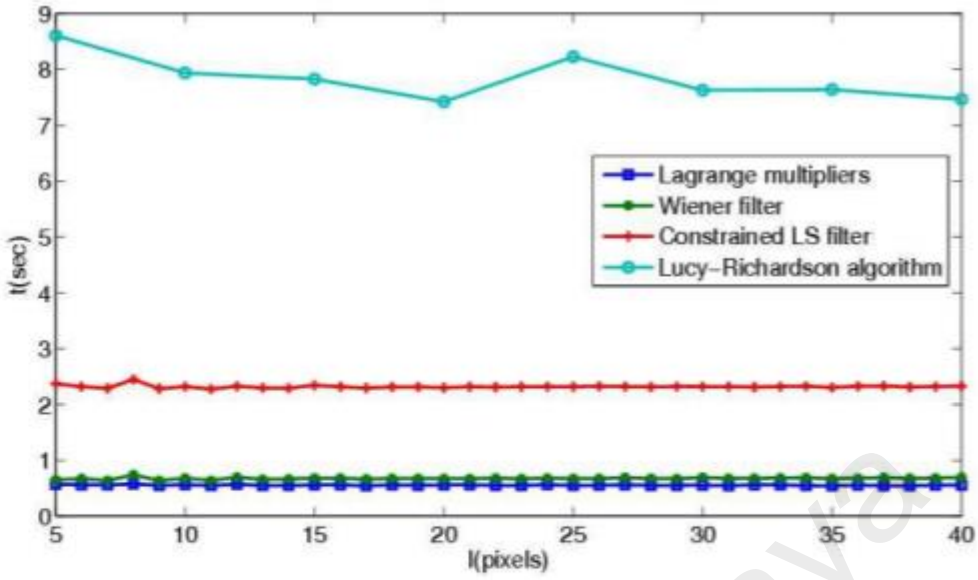

Figure 2.7.1 Computation Time vs Length of motion (Stojanovic et al., 2012)

2.8 Image Quality Assessment Techniques using SSIM

In this study, the image quality assessment (IQA) techniques is presented the method relates the correlation between objective scores and subjective evaluations. Basically, in the subjective IQA, humans are the evaluator of the image quality.

Observers are shown with an image and requested to input the score on a scale from 1 to 5 as shown in Table 2.4. The accumulated scores are then averaged to compute the mean opinion score (MOS). Generally, subjective IQA is not only expensive and troublesome in obtaining meaningful outcomes but also time consuming thus completely impracticable for real time processing.

Table 2.5 Mean Opinion Score (MOS) (Nisha, 2013)

1	2	3	4	5
Very Poor Quality	Poor Quality	Good Quality	Very Good Quality	Excellent Quality

On the other hand, objective IQA can be categorized into full reference (FR) model, no reference (NR) model, and reduced reference (RR) model, depending on the availability of the original image. FR model can be classified into simple statistical error metrics and human visual system feature based metrics.

Simple statistical error metrics include mean square error (MSE), peak signal to noise ratio (PSNR), average difference (AD), maximum difference (MD), and mean absolute error (MAE). These metrics are generally mathematical simple and tractable however they do not associate very well with the perceived quality since characteristics of human visual system (HVS) are not integrated into their models.

Human visual system featured based metrics include structural similarity index (SSIM) and mean structural similarity index (MSSIM). SSIM index measures the similarity of luminance, contrast, and structural between original image and degraded image whereas MSSIM index is the mean of SSIM.

This study shows that full reference metrics such as SSIM and MSSIM are more effective than PSNR and MSE as these metrics tend to become unstable in the presence of significant degradation (Nisha, 2013).

Experimental results show that MSE and PSNR are very fast and easy to implement but incapable of assessing image quality across different types of distortion. On the other hand, SSIM is capable of assessing image quality accurately across different types of distortion except highly blurred image (C.Sasi varnan, 2011).

CHAPTER 3: RESEARCH METHODOLOGY

3.1 Flow Chart of Image Degradation/Restoration

The flowchart of the image degradation and restoration method is shown. As shown in Figure 3.1.1, the original image is degraded by motion blur with length and angle of motion. This is accomplished by convoluting the PSF with the original image. Next, the several image restoration techniques are applied. The image quality metric is then applied on the restored images.

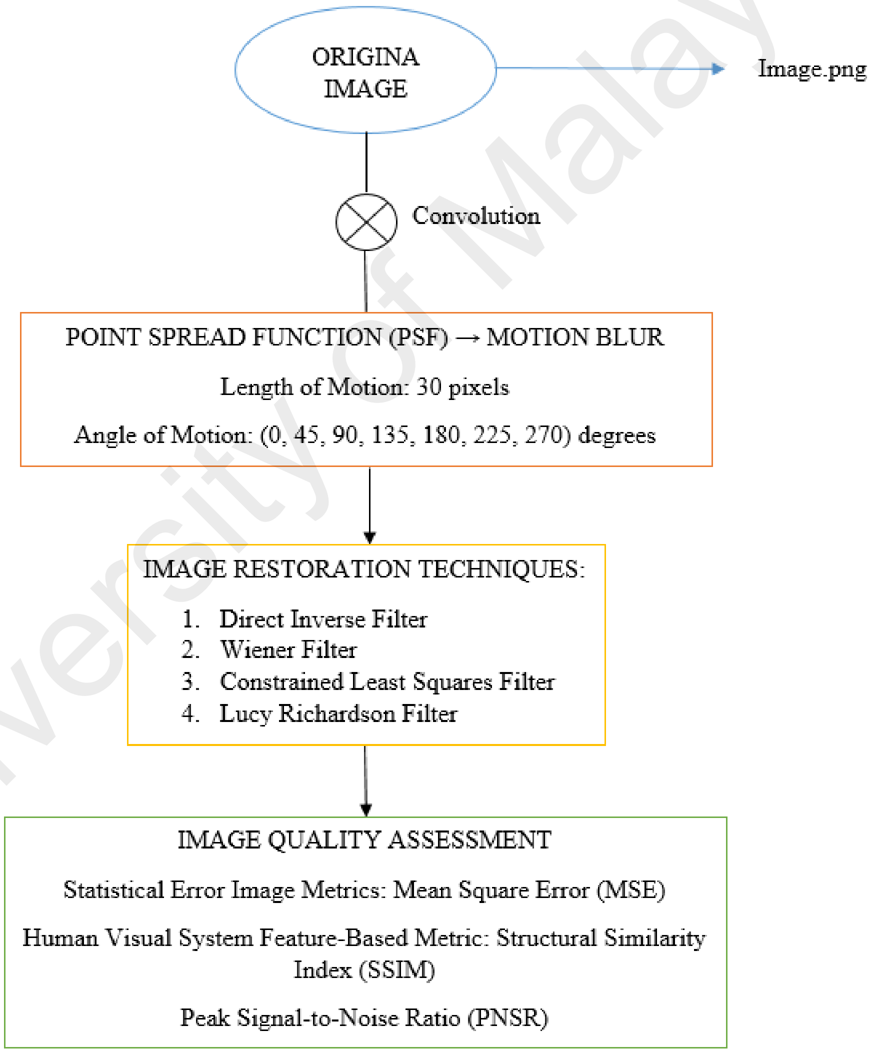

Figure 3.1.1 Flow Chart of Images Degradation/Restoration

3.2 Blur Model

When a camera moves along a certain direction and across a certain distance during exposure time then every point of the original scene is mapped onto several pixels of the recorded image. This phenomena gives rise to a recorded image that is motion blurred.

Motion blur is identified by two parameters, namely angle and length (Moghaddam & Jamzad, 2006). The motion blur effect is a filter that makes the image appear to be moving by adding a blur in a specific direction. The motion can be controlled by angle or direction (0 to 360 degrees) and/or by length or distance in pixels (0 to 999), based on the software used. Basically the angle describes the motion direction whilst the length describes the relative motion involved between the camera and scene during the exposure time. In addition, the angle is measured in degrees while the length is quantified in pixels.

In spatial domain, h(x,y) is referred to as the point spread function (PSF), a term that arises to characterized the spread out of a point of light (Gonzalez, Woods, & Eddins, 2010). In the frequency domain, the Fourier transform of h(x,y) is called the Optical transfer function (OTF). In other words, PSF is the inverse Fourier transform of OTF.

3.3 Point Spread Function

The PSF of motion blur is a spatially invariant. It means the blurring takes place the exact same way at every spatial location. Point spread function that are spatially variant include but not limited to rotational blur, local blur, etc. are beyond the scope of this research project. The PSF of motion blur is, in fact, a line segment through the origin and the total sum of the PSF coefficients is 1. Thus, the intensity is 1/L along the line segment and zero elsewhere.

The general PSF of the motion blur is mathematically formulated as follows:

$$h(m,n;L,\varphi) = \begin{cases} \frac{1}{L} & if\ \sqrt{m^2+\ n^2}\ \leq \frac{L}{2}\ and\ \frac{m}{n} = \ -\tan\varphi \\ 0 & elsewhere \end{cases}$$

Where m and n are the PSF pixel coordinates. Figure 3.3.1 illustrates the PSF obtained with application of above equation for linear motion for length of 30 pixels and at an angle of zero degrees, while Figure 3.3.9 shows the effect of motion blurring on the colored chips image. The filter spreads the effect of the neighboring pixels in the direction of motion.

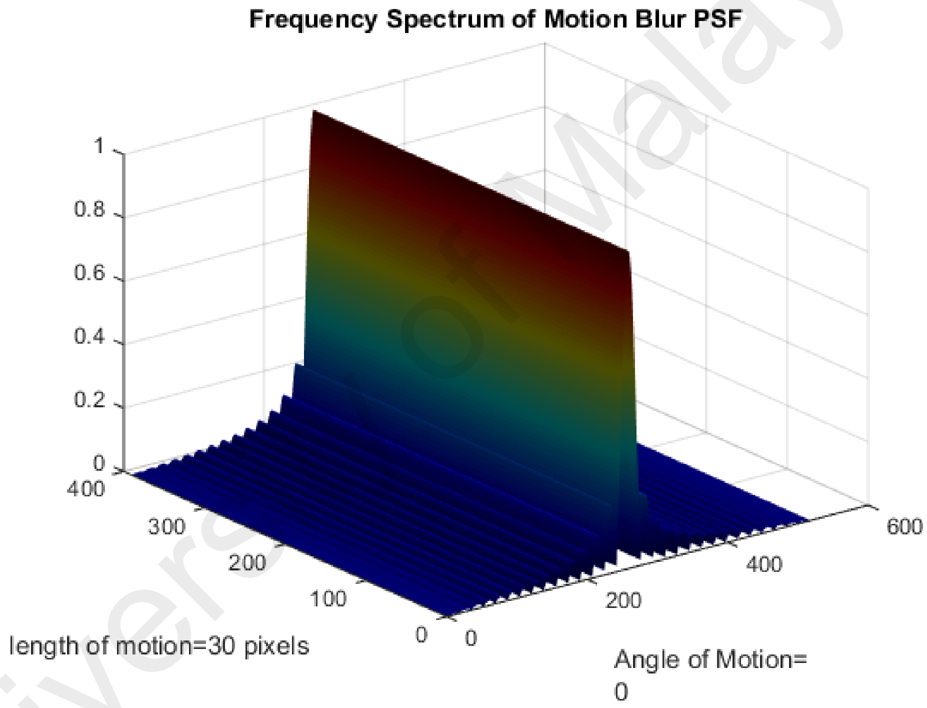

Figure 3.3.1 Frequency Response of Motion Blur with L = 30 pixels and θ = 0°

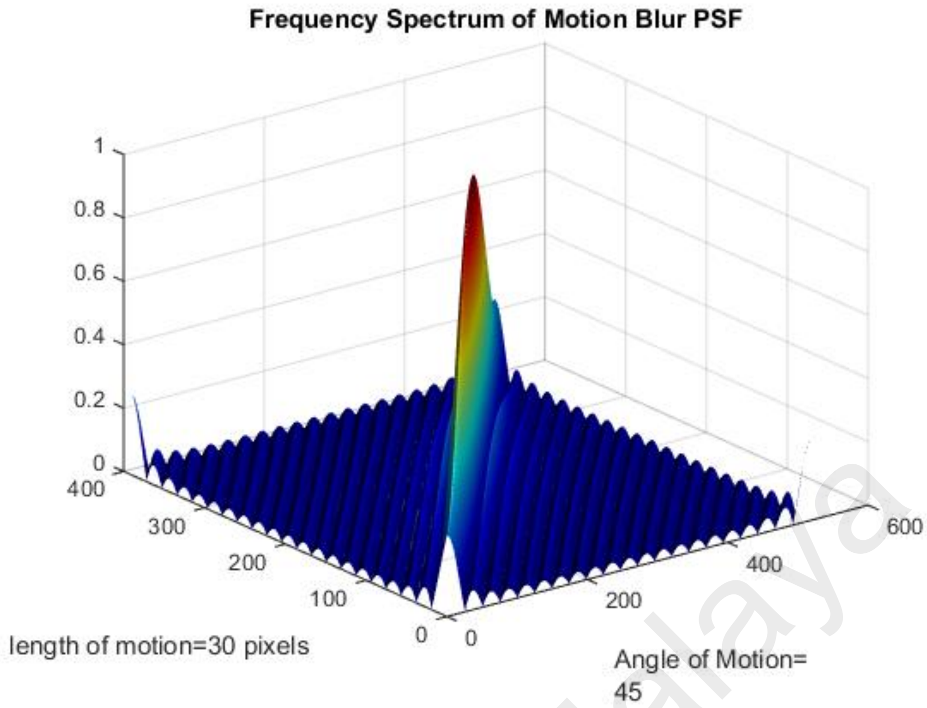

Figure 3.3.2 Frequency Response of Motion Blur with L = 30 pixels and θ = 45°

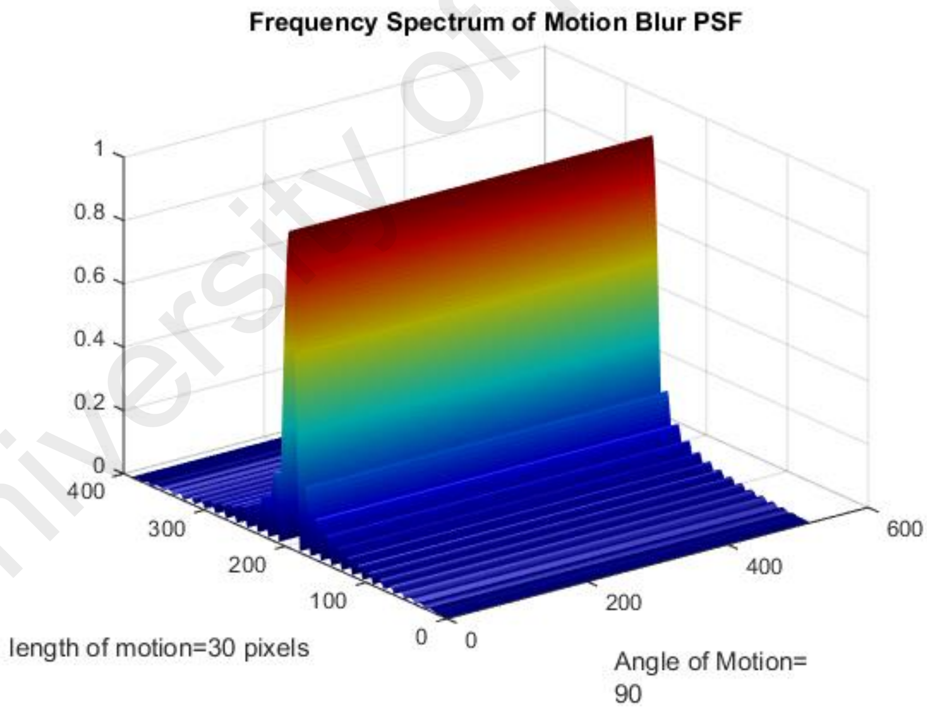

Figure 3.3.3 Frequency Response of Motion Blur with L = 30 pixels and θ = 90°

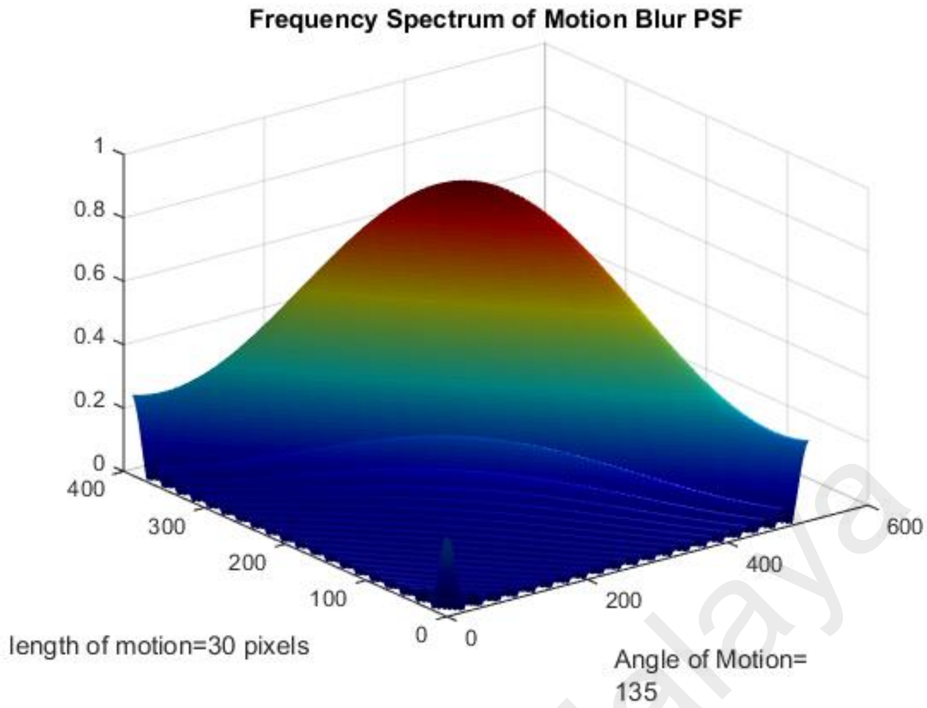

Figure 3.3.4 Frequency Response of Motion Blur with L = 30 pixels and θ = 135°

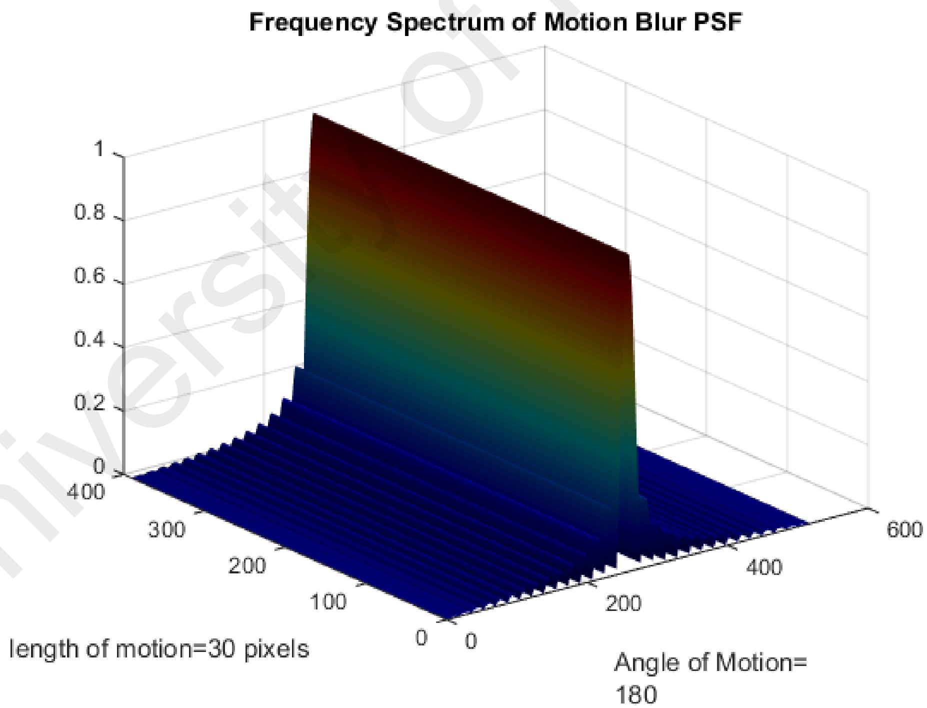

Figure 3.3.5 Frequency Response of Motion Blur with L = 30 pixels and θ = 180°

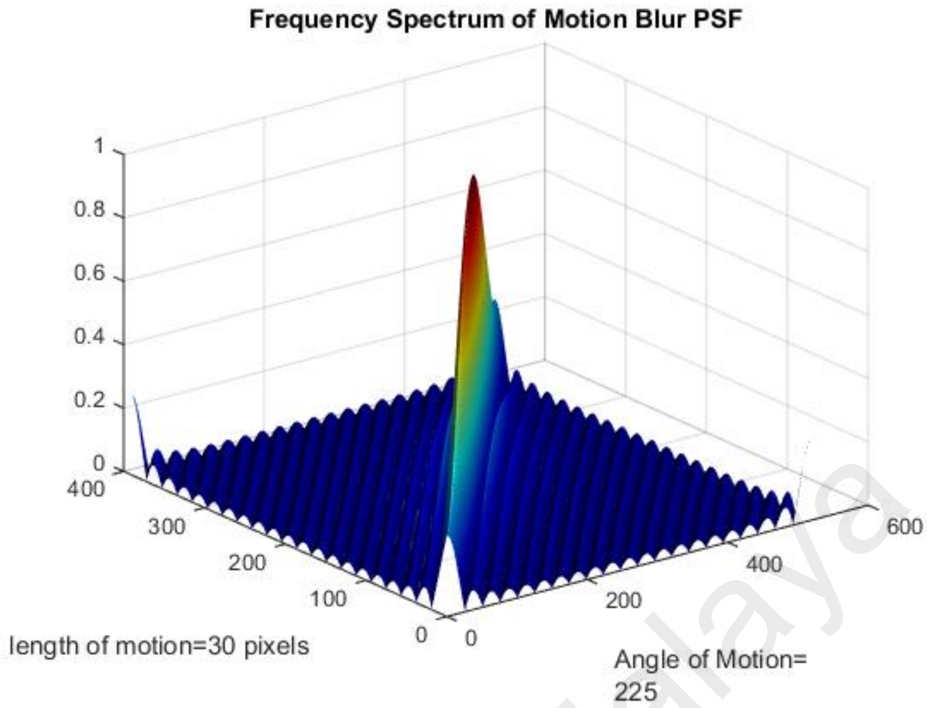

Figure 3.3.6 Frequency Response of Motion Blur with L = 30 pixels and θ = 225°

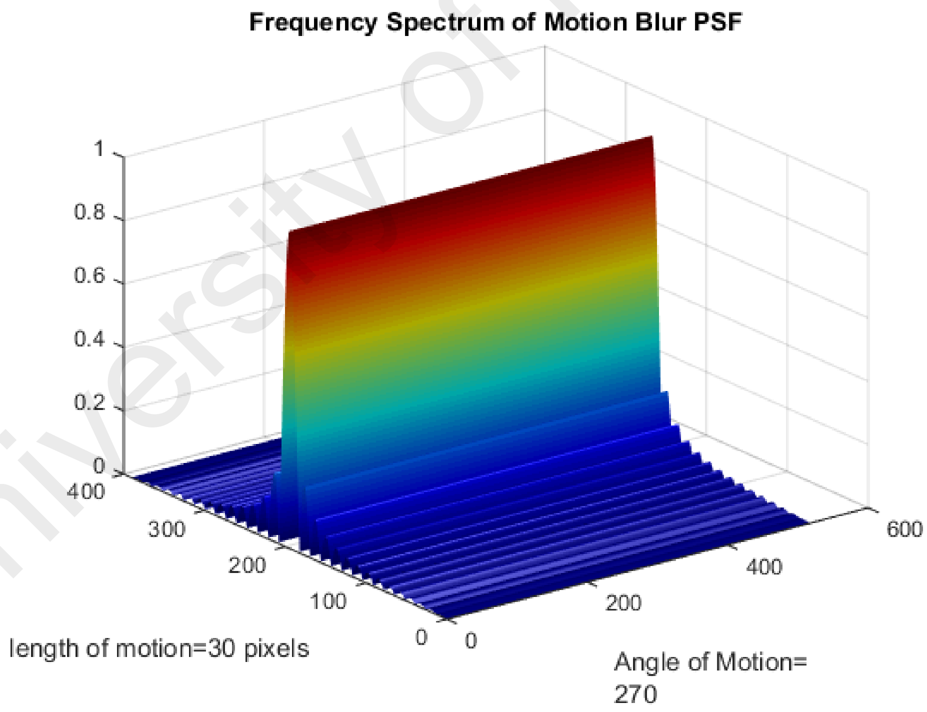

Figure 3.3.7 Frequency Response of Motion Blur with L = 30 pixels and θ = 270°

The result of the motion blurring in the modelled as the convolution of the original image $f(x, y)$ with the PSF $h(x, y)$ and is mathematically formulated as follows (Sngulagi, 2015).

$$g(x, y) = f(x, y) * h(x, y)$$

Figure 3.3.8 shown the original image while Figure 3.3.9 till Figure 3.3.15 illustrate the convolution of original image with PSF.

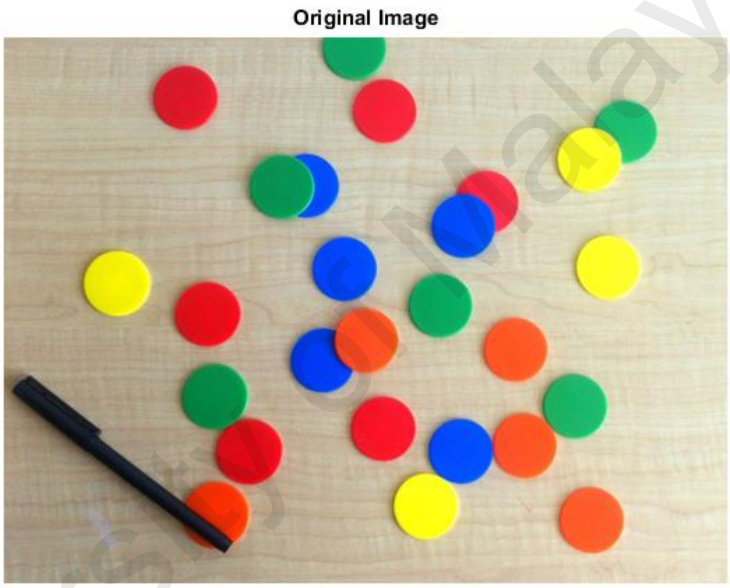

Figure 3.3.8 Original Image

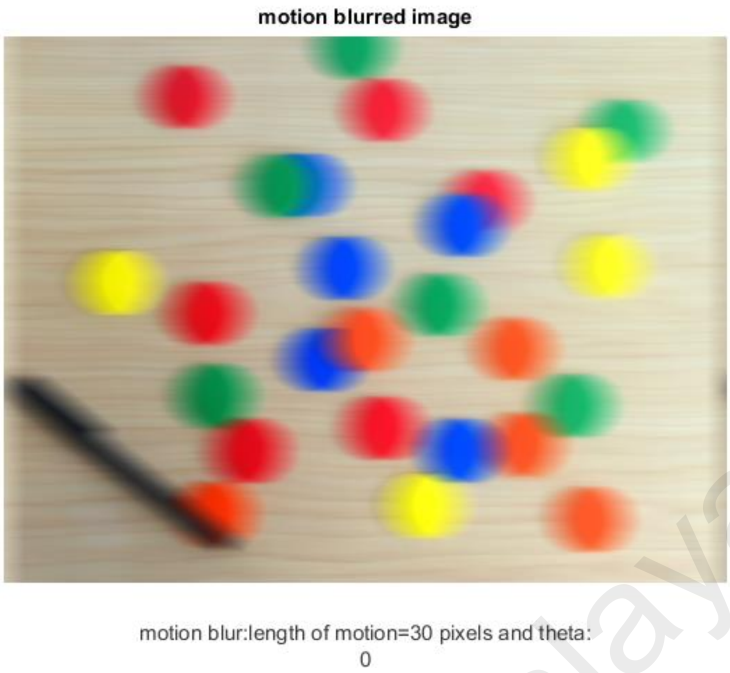

Figure 3.3.9 Motion Blurred Image with L = 30 and θ = 0°

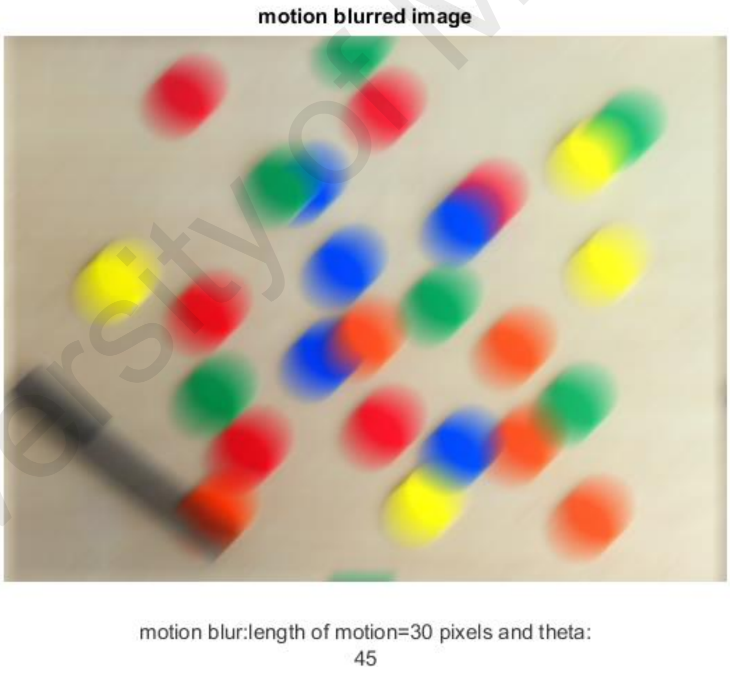

Figure 3.3.10 Motion Blurred Image with L = 30 and θ = 45°

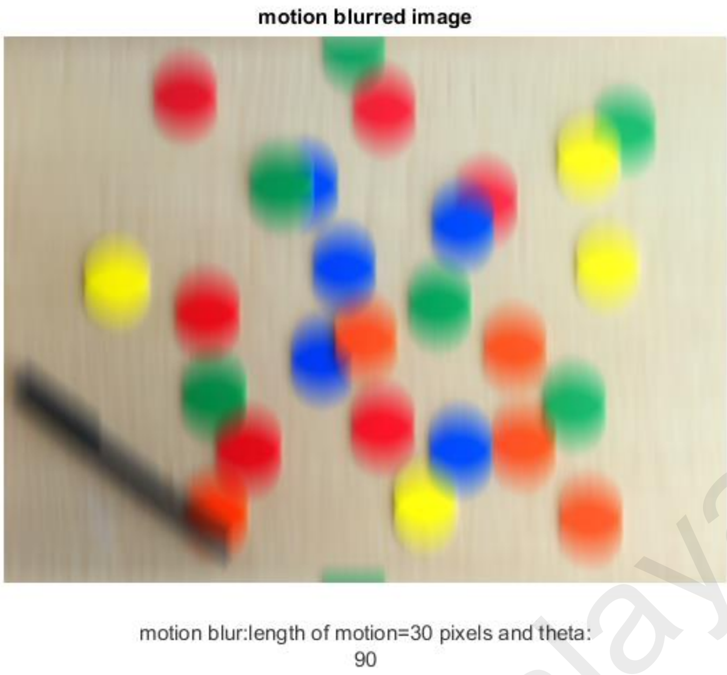

Figure 3.3.11 Motion Blurred Image with L = 30 and θ = 90°

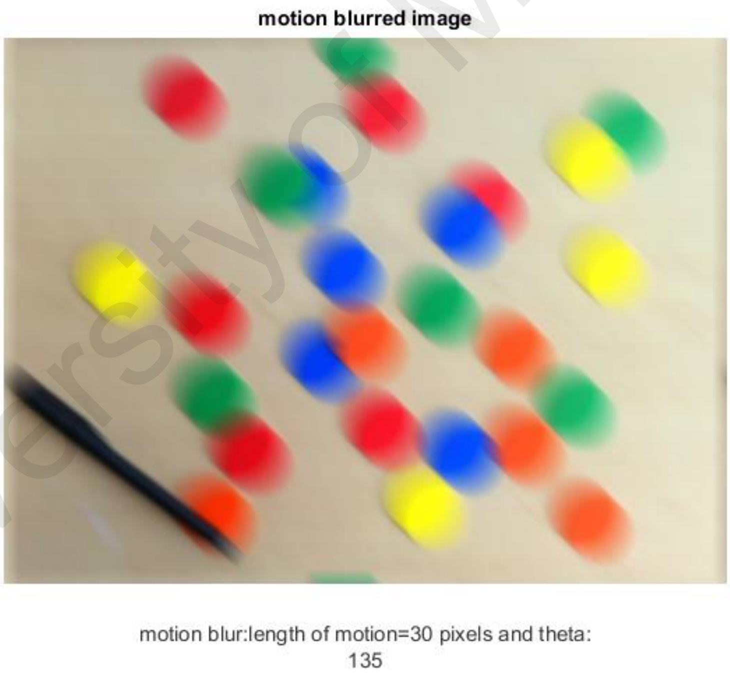

Figure 3.3.12 Motion Blurred Image with L = 30 and θ = 135°

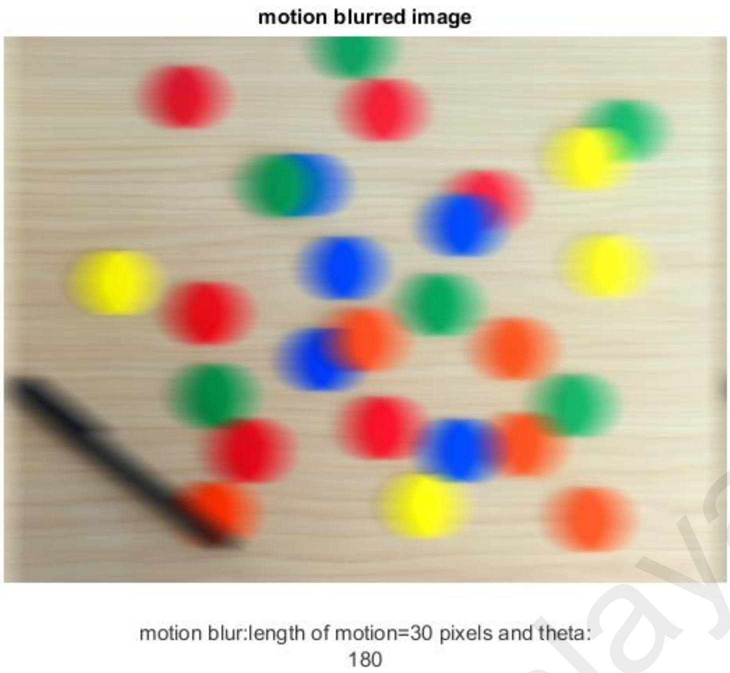

Figure 3.3.13 Motion Blurred Image with L = 30 and θ = 180°

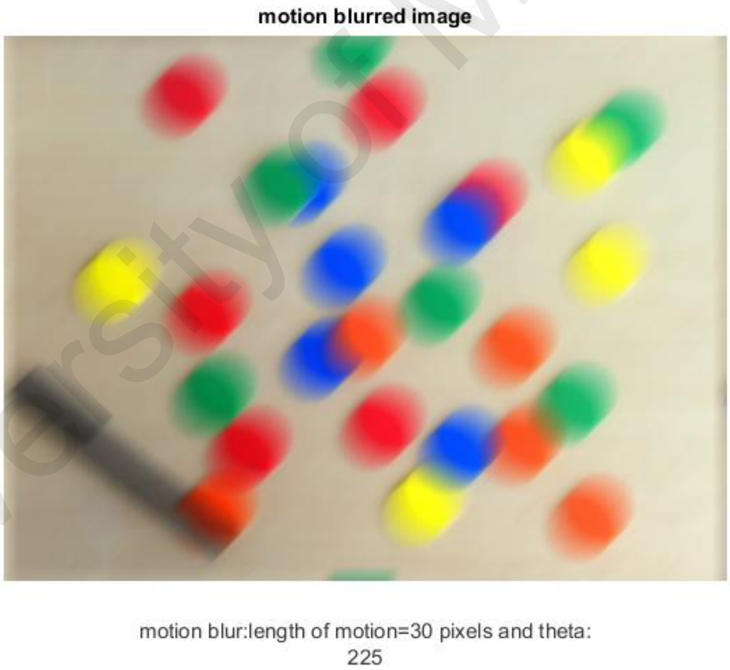

Figure 3.3.14 Motion Blurred Image with L = 30 and θ = 225°

Figure 3.3.15 Motion Blurred Image with L = 30 and θ = 270°

3.4 Image Quality Assessment (IQA)

Measurement of image quality is important for many image processing applications. Image quality assessment is closely related to image similarity assessment in which quality is based on the differences (or similarity) between a degraded image and the original, unmodified image. Image quality assessment (IQA) is defined as the estimation and evaluation of the perceptual quality of an image in a way associated with the human appreciation. IQA can be classified into two categories, namely subjective and objective methods. The former category is evaluated by humans whereas the latter category is evaluated by image quality metrics. Objective image quality metrics can be categorized into three different classes, namely full reference, reduced reference, and no reference, depending on the availability of the original image with which the restored image is to be compared with (C.Sasi varnan, 2011). In this research project, the full reference image quality metrics, namely Mean Squared Error (MSE), Peak Signal to Noise Ratio (PSNR), and Structural Similarity Index (SSIM) are employed to evaluate and estimate the quality of restored images.

3.4.1 Mean Squared Error (MSE)

Mean squared error (MSE) defines the difference between the original image and the restored image (Eskicioglu & Fisher, 1995). As well as, defines the cumulative squared error between the restored image and the restored image (Nisha, 2013). The mathematical definition for MSE is:

$$\text{MSE} = \frac{1}{M * N} \sum_{M\,N} [I_1(m,n) - I_2(m,n)]^2$$

Where M and N are the number of rows and columns in the original image and restored image. The lower the cumulative squared error between the images, the smaller the value of MSE. The greatest error free restoration is accomplished when the value of MSE is equal to zero.

3.4.2 Peak Signal-to-Noise Ratio (PSNR)

The PSNR block computes the peak signal-to-noise ratio, in decibels, between two images. This ratio is often used as a quality measurement between the original and a compressed image. A higher PSNR value simply means that the quality of the restored image is higher (C.Sasi varnan, 2011) PSNR is mathematically formulated as follows:

$\text{PSNR} = 10\ log_{10} \left(\frac{P^2}{MSE}\right)$; P = maximum pixel value

It is interesting to note that a small mean square error will result in a high peak signal to noise ratio and vice versa.

3.4.3 Structural Similarity Index (SSIM)

SSIM index is a perceptual metric that measures the similarity between the restored image and the original image. SSIM index measures the similarity of luminance, contrast, and structural between the two input images (Li & Bovik, 2010) . The luminance, contrast, and structural functions of the SSIM index are formulated individually as follows (Kudelka Jr, 2012):

$$\text{Luminance, l(x, y)} = \frac{2m_x m_y + C_1}{m_x^2 + m_x^2 + C_1}$$

$$\text{Contrast, c(x, y)} = \frac{2\sigma_x \sigma_y + C_2}{\sigma_x^2 + \sigma_y^2 + C_2}$$

$$\text{Structural, s(x, y)} = \frac{\sigma_{xy} + C_3}{\sigma_x \sigma_y + C_3}$$

Where m_x and m_y represent the means of original image and restored image, respectively;σ_x and σ_y are the standard deviations of original image and restored image, respectively; σ_{xy} is the covariance between original image and restored image; C_1, C_2 and C_3 are constants that stabilize the computations when the denominators become small.

The combination of the luminance, contrast, and structural functions yields a general form of SSIM index as follows:

$$\text{SSIM (x, y)} = \frac{(2m_x m_y + C_1)(2\sigma_x \sigma_y + C_2)}{(m_x^2 + m_x^2 + C_1)(\sigma_x^2 + \sigma_y^2 + C_2)}$$

SSIM index is a maximum (1) if and only if the original image equates restored image (Dosselmann & Yang, 2008).

3.5 Image Restoration Techniques

3.5.1 Direct Inverse Filter

Direct inverse filter computes an optimal estimate $\hat{F}(u,v)$ of the original image $F(u,v)$ simply dividing the degraded image $G(u,v)$ by the degradation function $H(u,v)$as follows:

$$\hat{F}(u,v) = \frac{G(u,v)}{\mathrm{H}(u,v)}$$

Substitute $G(u,v) with\ F(u,v)\ H(u,v) + N(u,v)$:

$$\hat{F}(u,v) = \frac{F(u,v)H(u,v) + N(u,v)}{\mathrm{H}(u,v)}$$

$$\hat{F}\ (u,v) = \frac{F(u,v)H(u,v)}{\mathrm{H}(u,v)} + \frac{N(u,v)}{\mathrm{H}(u,v)}$$

$$\hat{F}(u,v) = F(u,v) + \frac{N(u,v)}{\mathrm{H}(u,v)}$$

It is interesting to note that the direct inverse filter can recover a degraded image exactly in the absence of noise. However, in the event that the noise is unknown, then it is impossible for a direct inverse filter to reconstruct the degraded image. Furthermore, in the event that the degradation function has zero or absolute small values, then the noise can easily dominate the estimate $\hat{F}(u,v)$.

In a nutshell, the direct inverse filter makes no explicit for managing noise and tends to allow noise to dominate over the estimate in the process of restoration.

3.5.2 Wiener Filter

Wiener filter is an enhanced image restoration technique that integrates not only the degradation function but also statistical properties of noise and original image in the reconstruction process.

Wiener filter obtains an optimal estimate $\hat{f}(x,y)$ of the original image $f(x,y)$ by minimizing the mean square error (MSE) between them on the assumption that the blur and the original image are uncorrelated. The detailed derivation of Weiner filter is as follows:

$$e^2 = E\left[\left|f(x,y) - \hat{f}(x,y)\right|^2\right]$$

$$e^2 = E[|f(x,y) - g(x,y) * w(x,y)|^2]$$

Convert the statistical error function to frequency domain by applying Fourier transform onto each the corresponding terms:

$$e^2 = E[|F(u,v) - F(u,v)W(u,v)|^2]$$

Apply $G(u,v) = F(u,v)H(u,v) + N(u,v)$ into the statistical error function above to obtain:

$$e^2 = E[|F(u,v) - (F(u,v)H(u,v) + N(u,v))W(u,v)|^2]$$

$$e^2 = E[|F(u,v) - F(u,v)H(u,v)W(u,v) - N(u,v))W(u,v)|^2]$$

$$e^2 = E[|F(u,v)(1 - W(u,v)H(u,v)) - N(u,v)W(u,v)|^2]$$

Apply complex conjugate formula, $|z|^2 = z\bar{z} = \bar{z}z$:

$$e^2 = E\left[(F(u,v)\left(1 - W(u,v)H(u,v)\right) - N(u,v)W(u,v))\overline{(F(u,v)(1 - W(u,v)H(u,v)) - N(u,v)W(u,v))}\right]$$

$$e^2 = E\left[\left(F(u,v)\left(1 - W(u,v)H(u,v)\right) - N(u,v)W(u,v)\right)\overline{(F(u,v)}\;\overline{\left(1 - W(u,v)H(u,v)\right)} - \overline{N(u,v)W(u,v)}\;\right]$$

$$\begin{aligned} e^2 = E\Big[\Big(&F(u,v)\overline{F(u,v)}\left(1 - W(u,v)H(u,v)\right)\overline{\left(1 - W(u,v)H(u,v)\right)} \\ &- F(u,v)\left(1 - W(u,v)H(u,v)\right)\overline{N(u,v)W(u,v)} \\ &- \overline{(F(u,v)}\overline{\left(1 - W(u,v)H(u,v)\right)}N(u,v)W(u,v) \\ &+ W(u,v)\overline{W(u,v)}\;N(u,v)\overline{N(u,v)}\Big)\Big] \end{aligned}$$

The noise, $N(u,v)$is assumed to be independent of the original image $F(u,v)$, hence:

$$E\left[\overline{F(u,v)}\;F(u,v)\right] = E\left[\overline{N(u,v)}\;F(u,v)\right] = 0$$

Apply the assumption that the noise and the original image are uncorrelated into the statistical error function:

$$\begin{aligned} e^2 = E\Big[&F(u,v)\overline{F(u,v)}\left(1 - W(u,v)H(u,v)\right)\overline{\left(1 - W(u,v)H(u,v)\right)} \\ &+ W(u,v)\overline{W(u,v)}\;N(u,v)\overline{N(u,v)}\;\Big] \end{aligned}$$

In addition, the power spectral densities of the noise and original image are defined as follows:

$$S_F(u,v) = |F(u,v)|^2$$

$$S_N(u,v) = |N(u,v)|^2$$

Therefore,

$$e^2 = E\left[S_F(u,v)\big(1 - W(u,v)H(u,v)\big)\overline{\big(1 - W(u,v)H(u,v)\big)} + W(u,v)\overline{W(u,v)}\,S_N(u,v)\ \right]$$

Find the minimum value of the function by differentiating the statistical error function with respect to Wiener filter, $W(u,v)$:

$$\frac{d\varepsilon}{dW} = -\,H(u,v)\overline{\big(1 - W(u,v)H(u,v)\big)}S_F(u,v) + \overline{W(u,v)}\,S_N(u,v)$$

$$\frac{d\varepsilon}{dW} = \overline{W(u,v)}\,S_N(u,v) - \ H(u,v)\overline{\big(1 - W(u,v)H(u,v)\big)}S_F(u,v)$$

Set derivative equal to zero and solve for wiener filter, $W(u,v)$:

$$\overline{W(u,v)}\,S_N(u,v) - \ H(u,v)\overline{\big(1 - W(u,v)H(u,v)\big)}S_F(u,v) = 0$$

$$\overline{W(u,v)}\,S_N(u,v) = H(u,v)\overline{\big(1 - W(u,v)H(u,v)\big)}S_F(u,v)$$

$$\overline{W(u,v)}\,S_N(u,v) = S_F(u,v)\,H(u,v) - S_F(u,v)\,H(u,v)\overline{H(u,v)W(u,v)}$$

$$S_N(u,v) = \frac{S_F(u,v)H(u,v)}{\overline{W(u,v)}} - \frac{S_F(u,v)\,H(u,v)\overline{H(u,v)W(u,v)}}{\overline{W(u,v)}}$$

$$S_N(u,v) = \frac{S_F(u,v)H(u,v)}{\overline{W(u,v)}} - S_F(u,v)\,H(u,v)\overline{H(u,v)}$$

$$S_N(u,v) + S_F(u,v)\,H(u,v)\overline{H(u,v)} = \frac{S_F(u,v)H(u,v)}{\overline{W(u,v)}}$$

$$\overline{W(u,v)} = \frac{S_F(u,v)H(u,v)}{S_N(u,v) + S_F(u,v)\,H(u,v)\overline{H(u,v)}}$$

$$\overline{W(u,v)} = \frac{S_F(u,v)H(u,v)}{S_N(u,v) + S_F(u,v)\,H(u,v)\overline{H(u,v)}} \times \frac{\frac{1}{S_F(u,v)}}{\frac{1}{S_F(u,v)}}$$

$$\overline{W(u,v)} = \frac{H(u,v)}{\frac{S_N(u,v)}{S_F(u,v)} + H(u,v)\overline{H(u,v)}}$$

$$W(u,v) = \frac{\overline{H(u,v)}}{\frac{S_N(u,v)}{S_F(u,v)} + H(u,v)\overline{H(u,v)}}$$

$$W(u,v) = \frac{\overline{H(u,v)}}{\frac{S_N(u,v)}{S_F(u,v)} + H(u,v)\overline{H(u,v)}} \times \frac{H(u,v)}{H(u,v)}$$

$$W(u,v) = \frac{\overline{H(u,v)}H(u,v)}{\frac{S_N(u,v)}{S_F(u,v)} + H(u,v)\overline{H(u,v)}} \times \frac{1}{H(u,v)}$$

$$W(u,v) = \frac{|H(u,v)|^2}{\frac{S_N(u,v)}{S_F(u,v)} + |H(u,v)|^2} \times \frac{1}{H(u,v)}$$

$$\hat{F}(u,v) = W(u,v) \times G(u,v)$$

$$\hat{F}(u,v) = \left[\frac{|H(u,v)|^2}{\frac{S_N(u,v)}{S_F(u,v)} + |H(u,v)|^2} \times \frac{1}{H(u,v)}\right] \times G(u,v)$$

Where

$\hat{F}(u,v)$ = optimal estimate of original image $F(u,v)$

$H(u,v)$ = the degradation/blurring/PSF/OTF function

$|H(u,v)|^2 = \overline{H(u,v)}\,H(u,v)$

$\overline{H(u,v)}$ = the complex conjugate of $H(u,v)$

$S_F(u,v) = |F(u,v)|^2$ = the power spectrum of the original image

$S_N(u,v) = |N(u,v)|^2$= the power spectrum of the additive noise

Power spectrum density (PSD) or power spectrum of a signal describes the average signal power per spatial frequency (u,v). The power spectral densities of original image and additive noise are represented by $S_F(u,v)$ and $S_N(u,v)$ respectively.

The ratio $S_N(u,v)/S_F(u,v)$ is known as the noise to signal power ratio. It is important to note that in the absence of noise, the power spectrum of noise, $S_N(u,v)$ is zero, hence, the noise to signal power ratio becomes zero as well. In other words, the Wiener filter reduces or approximates to a direct inverse filter in the absence of noise.

Furthermore, the power spectrum of the noise is determined by the noise variance only for all spatial frequencies due to the assumption that the noise is independent of the original Image, thus has zero mean.

$$S_N(u,v) = \sigma^2 for\ all\ (u,v)$$

However, the estimation of power spectrum of the original image is often challenging since the original image in practical case is obviously unavailable. Thus, periodogram is an approach commonly used to estimate the power spectrum of the original image by determining the power spectrum of the degraded image and compensating for the variance of the noise σ_n^2.

$$S_F(u,v) \approx S_G(u,v) - \sigma_n^2 \approx \frac{1}{NM}\overline{G(u,v)}G(u,v) - \sigma_n^2$$

Last but not least, it is important to note that even in the event that the noise to signal power ratio is unknown, the optimal estimate of the original image can still be obtained by varying the constant ratio and observing the restored outcomes.

3.5.3 Constrained Least Squares (CLS) Filter

Constrained least squares (CLS) filter is another image restoration technique, the CLS filter requires only information about the length and theta of blur in the process of image restoration by applying Laplacian filter and imposing constraint so that the sum of squares of the Laplacian values at each pixels is minimal.

Apply Laplacian filter with constraint so that the sum of the squares of the Laplacian values at each pixel position is minimal

$$\sum_{x=0}^{M-1}\sum_{y=0}^{N-1}[\Delta^2 f(x,y)]^2 = (Lf)^T (Lf) = minimal$$

Where

Constraint:

$$\left|g - H\hat{f}\right|^2 = |n|^2$$

$$|n|^2 = n^T n = \varepsilon$$

$$\left|g - H\hat{f}\right|^2 = \left(g - H\hat{f}\right)^T\left(g - H\hat{f}\right)$$

$$\left(g - H\hat{f}\right)^T\left(g\varepsilon - H\hat{f}\right) = \varepsilon$$

Minimal $(Lf)^T(Lf)$ with the constraint of $\left(g - H\hat{f}\right)^T\left(g\varepsilon - H\hat{f}\right) = \varepsilon$

$$Let\ a(x,y) = \sum_{x=0}^{M-1}\sum_{y=0}^{N-1}[\Delta^2 f(x,y)]^2 = (Lf)^T (Lf) = minimal$$

$$And\ b(x,y) = \varepsilon = \left(g - H\hat{f}\right)^T \left(g\varepsilon - H\hat{f}\right)$$

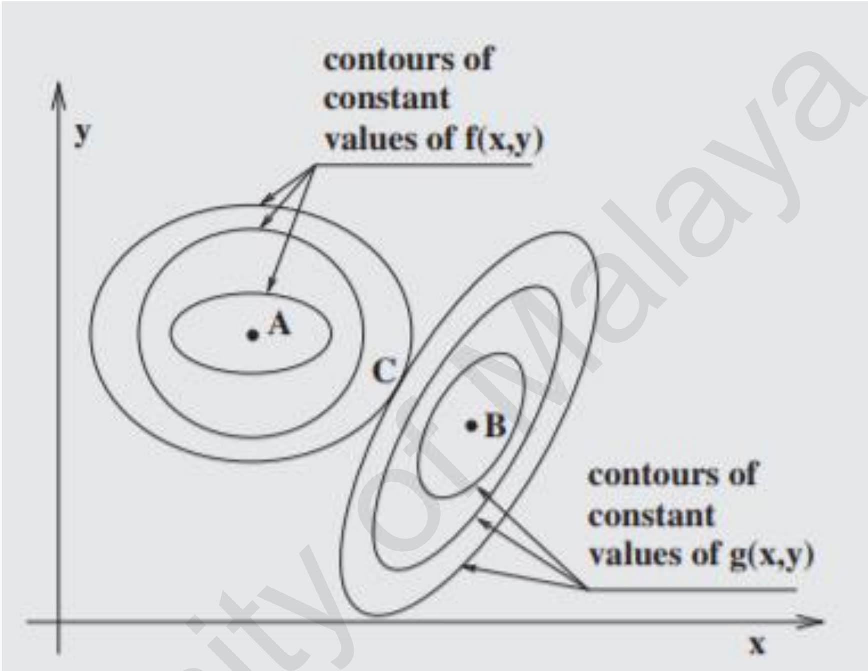

Figure 3.5.1 Satisfaction of Two Incompatible Equations

Figure 4.3.1 illustrates that in the (x, y) plane, $a(x, y)$ is exactly satisfied at point A whereas is exactly satisfied at point B. Hence, it is an uphill task to satisfy both $a(x, y)$ and $b(x, y)$ exactly for the same value of (x, y). However, the point where the two isocontour of the functions just touch is the point where minimal total violation of two constraints takes place.

As the contours grow away from point A, the values function$|a(x, y)|$ takes become greater. Similarly, as the contours grow away from point B, function $|b(x, y)|$ takes greater values.

Point C, where the values of $|a(x, y)|$ and $|b(x, y)|$ are as small as possible, must be the point where an isocontour around A just touches an isocontour around B, without crossing each other(Petrou & Petrou, 2010). When two curves just touch each other, their tangents become parallel. The tangent vector to a curve along with a = constant is ∇a and the tangent vector to a curve along which b = constant is ∇b. The two tangent vectors do not need to have the same magnitude for the minimum violation of the constraints. It is sufficient for them to have the same orientation. Therefore, point C is determined by the solution of equation $\nabla a + \Lambda \nabla b$ where Λ is the Lagrange multiplier, an arbitrary constant that takes care of the probably dissimilar magnitudes of the two vectors. In other words, the solution to the simultaneous satisfaction of two incompatible equations is the solution of the differential set of equations as follows:

$$\nabla \hat{f} + \Lambda \nabla \varepsilon = 0$$

Substitute $\varepsilon = \left(g - H\hat{f}\right)^T \left(g\varepsilon - H\hat{f}\right)$

$$\frac{d}{df}\left[L^T \hat{f}^T L\hat{f} + \Lambda\left(g - H\hat{f}\right)^T \left(g\varepsilon - H\hat{f}\right)\right] = 0$$

$$\frac{d\hat{f}^T a}{d\hat{f}} = a; \frac{db^T \hat{f}}{d\hat{f}} = b; \frac{d\hat{f}^T A\hat{f}}{d\hat{f}} = (A + A^T)\hat{f}$$

$$\frac{d}{df}\left[\hat{f}^T L^T L\hat{f} + \Lambda\left(g^T g - g^T H\hat{f} - H^T g\hat{f}^t + \hat{f}^T H^T H\hat{f}\right)\right] = 0$$

$$(L^T L + L^T L)\hat{f} + \Lambda\left[0 - H^T g - H^T g + (H^T H + H^T H)\hat{f}\right] = 0$$

$$2L^T L\hat{f} - 2\Lambda H^T g + 2\Lambda H^T H\hat{f} = 0$$

$$2L^T L\hat{f} + 2\Lambda H^T H\hat{f} = 2\Lambda H^T g$$

$$2\hat{f}(L^T L + \lambda H^T H) = 2\lambda H^T g$$

$$\hat{f} = \frac{2\lambda H^T g}{2(L^T L + \lambda H^T H)}$$

$$\hat{f} = \frac{\lambda H^T g}{(L^T L + \lambda H^T H)}$$

$$Let\ y = \frac{1}{\lambda}$$

$$\hat{f} = \frac{H^T g}{y L^T L + H^T H}$$

$$\hat{f} = \frac{H^T g}{H^T H + y L^T L}$$

$$\hat{F}(u,v) = \frac{H^T(u,v) G(u,v)}{H^T(u,v) H(u,v) + y L^T(u,v) L(u,v)}$$

$$\hat{F}(u,v) = G(u,v)\ \frac{H^T(u,v)}{H^T(u,v) H(u,v) + y L^T(u,v) L(u,v)} \frac{H(u,v)}{H(u,v)}$$

$$\hat{F}(u,v) = G(u,v)\ \frac{H^T(u,v) H(u,v)}{H^T(u,v) H(u,v) + y L^T(u,v) L(u,v)} \frac{1}{H(u,v)}$$

$$\hat{F}(u,v) = \left[\frac{H^T(u,v) H(u,v)}{H^T(u,v) H(u,v) + y L^T(u,v) L(u,v)} \frac{1}{H(u,v)}\right] G(u,v)$$

$$\hat{F}(u,v) = \left[\frac{|H(u,v)|^2}{|H(u,v)|^2 + y|L(u,v)|^2} \frac{1}{H(u,v)}\right] G(u,v)$$

Where

$\hat{F}(u,v)$ = The optimal estimate of the original image

$H(u,v)$ = The degradation/blurring/PSF/OTF function

$|H(u,v)|^2 = H^T(u,v)H(u,v)$

$H^T(u,v)$ = Transpose of $H(u,v)$

$L(u,v)$ = Fourier transform of Laplacian filter, $l(u,v)$

$$l(u,v) = \begin{bmatrix} 0 & 1 & 0 \\ 1 & -4 & 1 \\ 0 & 1 & 0 \end{bmatrix}$$

3.5.4 Lucy Richardson (LR) Algorithm

Lucy Richardson (LR) algorithm, sometimes referred to as Richardson Lucy (RL) algorithm. is an iterative image restoration technique. It is interesting to note that actually LR algorithm is initially established to restore astronomical images that have been contaminated largely with Poisson noise however this iterative algorithm performs relatively well even for images that have been contaminated with other types of noise. Furthermore, LR algorithm does not require any knowledge about the original image. This feature makes LR algorithm a very practical image restoration technique because in actual scenarios more often than not the original image is unavailable.

Theoretically, LR algorithm is developed based on a Bayesian framework by maximizing the likelihood probability function iteratively as follows:

$$p(F|G) = p(G|F)\frac{p(F)}{p(G)}$$

Where $p(F|G)$ is the likelihood probability, $p(F|G))$ is the posterior probability, $p(F)$ is a model of the original image, and $p(G)$ is a model of the degraded image.

The likelihood probability for image modelled with Poisson process is mathematically formulated as follows:

$$p(G|F) = \prod_{u,v} \frac{[H(u,v) * F(u,v)]^{G(u,v)} e^{-[H(u,v)*F(u,v)]}}{G(u,v)!}$$

The likelihood probability above is maximized by minimizing the negative log likelihood as follows:

$$-log\ p(G|F) = \int_u^v \big[H(u,v) * F(u,v) - G(u,v) log\big[[H(u,v) * F(u,v)]\big]$$
$$+ log[G(u,v)]!\big] duv$$

$$J\big(F(u,v)\big) = \int_u^v \big[H(u,v) * F(u,v) - G(u,v) log[H(u,v) * F(u,v)]\big] duv$$

A small perturbation $p\hat{F}(u,v)$ is added to the original image $F(u,v)$ in order to compute the derivative of the function as follows:

$$J\left(F(u,v) + p\hat{F}(u,v)\right)$$
$$= \int_u^v \Big[H(u,v) * \big[F(u,v) + p\hat{F}(u,v)\big]$$
$$- G(u,v) log\left[H(u,v) * \left[F(u,v) + p\hat{F}(u,v)\right]\right]\Big] duv$$

$$J\left(F(u,v) + p\hat{F}(u,v)\right)$$
$$= \int_u^v \Bigg[H(u,v) * F(u,v) + p\left(H(u,v) * \hat{F}(u,v)\right)$$
$$- G(u,v) log\left[H(u,v) * F(u,v)\left[1 + p\frac{H(u,v) * \hat{F}(u,v)}{H(u,v) * F(u,v)}\right]\right]\Bigg] duv$$

$$J\left(F(u,v) + p\hat{F}(u,v)\right)$$

$$= \int_u^v \left[H(u,v) * F(u,v) + p\left(H(u,v) * \hat{F}(u,v)\right)\right.$$

$$\left. - G(u,v)log\left[H(u,v) * F(u,v) - \left[pG(u,v)\frac{H(u,v) * \hat{F}(u,v)}{H(u,v) * F(u,v)}\right]\right]\right] duv$$

$$J\left(F(u,v) + p\hat{F}(u,v)\right)$$

$$= J\big(F(u,v)\big)$$

$$+ p\int_u^v \left[\left(H(u,v) * \hat{F}(u,v)\right) - G(u,v)\frac{H(u,v) * \hat{F}(u,v)}{H(u,v) * F(u,v)}\right] duv$$

$$\int_u^v \left[\left(H(u,v) * \hat{F}(u,v)\right) - G(u,v)\frac{H(u,v) * \hat{F}(u,v)}{H(u,v) * F(u,v)}\right] duv$$

$$= \int_u^v \hat{F}(u,v)\left[\overline{H(u,v)} - \overline{H(u,v)} * \frac{G(u,v)}{H(u,v) * F(u,v)}\right] duv$$

$$\nabla J[F(u,v)] = H(-u,-v) * \left[1 - \frac{G(u,v)}{H(u,v) * F(u,v)}\right]$$

Set the derivative $\nabla J[F(u,v)] =$ to zero to obtain:

$$\int_u^v H(-u,-v)duv - H(-u,v)\frac{G(u,v)}{H(u,v)*F(u,v)} = 0$$

The PSF has an energy of one, thus:

$$H(-u,v) * \frac{G(u,v)}{H(u,v)*F(u,v)} = 1$$

Assume that the convergence ratio $\hat{F}^{p+1}(u,v)/\hat{F}^{p}(u,v) = 1$, then yields the following equation:

$$\hat{F}^{p+1}(u,v) = \hat{F}^{p}(u,v)\left[H(-u,v) * \frac{G(u,v)}{H(u,v)*F(u,v)}\right]$$

Convert to spatial domain:

$$\hat{f}_{k+1}(x,y) = \hat{f}_{k}(x,y)\ \left[H(-x,-y) * \frac{G(-x,-y)}{H(-x,-y)*F(-x,-y)}\right]$$

CHAPTER 4: RESULTS AND DISCUSSIONS

This chapter shows the results of the four methods used to restore the degraded image. The restored image is evaluated using the image quality metric discussed in the earlier chapters. A total of seven images is used in this experimented study. The degraded images are blurred with a fixed length of 30 pixels and with various angles of motion.

4.1 Direct Inverse Filter

Direct inverse filter is mathematically formulated as follows:

$$\hat{F}(u,v) = \frac{F(u,v)H(u,v) + N(u,v)}{H(u,v)}$$

However, in the absence of noise, the direct inverse filter reduces to:

$$\hat{F}(u,v) = \frac{F(u,v)H(u,v) + 0}{H(u,v)}$$

$$\hat{F}(u,v) = \frac{F(u,v)H(u,v)}{H(u,v)}$$

$$\hat{F}(u,v) = F(u,v)$$

Figure 4.1.1 Image Restoration using Direct Inverse Filter

Figure 5.1.1 illustrates and validates that a direct inverse filter is indeed an excellent image restoration technique. It is capable of recovering a motion blurred image exactly in the absence of noise. The MSE and PSNR of the restored image are $0.8133 * 10^{-6}$ and 109.0285 dB respectively. The MSE value indicated that the cumulative squared error between the restored image and the original image is extremely minimal while the high PSNR value indicates that the restored image presents a high quality image.

Figure 4.1.2 Restored image using Direct Inverse Filter at 0 degree

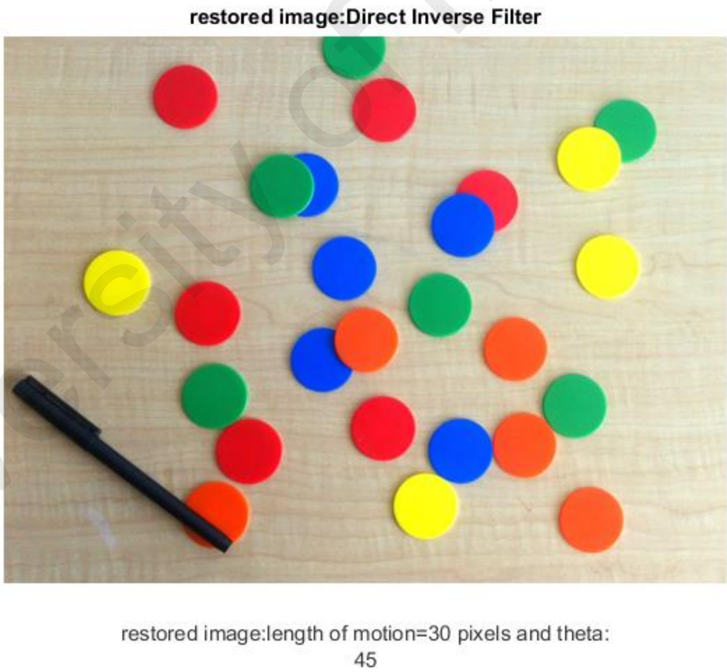

Figure 4.1.3 Restored image using Direct Inverse Filter at 45 degree

Figure 4.1.4 Restored image using Direct Inverse Filter at 90 degree

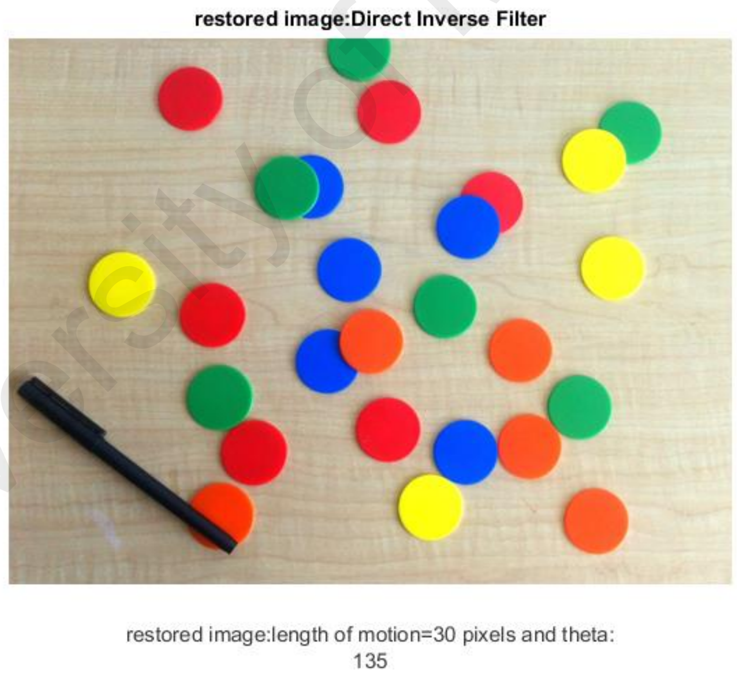

Figure 4.1.5 Restored image using Direct Inverse Filter at 135 degree

Figure 4.1.6 Restored image using Direct Inverse Filter at 180 degree

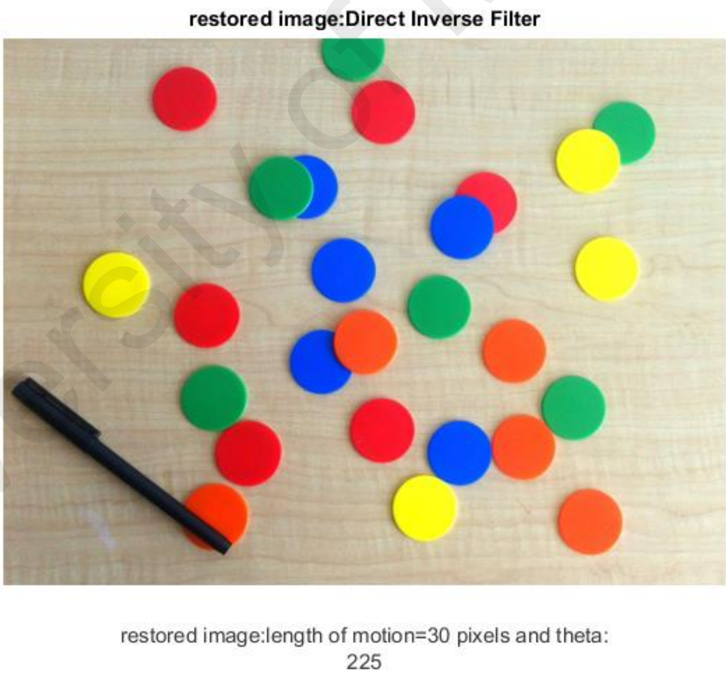

Figure 4.1.7 Restored image using Direct Inverse Filter at 225 degree

Figure 4.1.8 Restored image using Direct Inverse Filter at 270 degree

Table 4.1 MSE, PSNR and SSIM of Direct Inverse Filter

Direct Inverse Filter							
Theta	**0**	**45**	**90**	**135**	**180**	**225**	**270**
length	**30**	**30**	**30**	**30**	**30**	**30**	**30**
MSE	**$0.3254*10^{-6}$**	**$0.8133*10^{-6}$**	**$0.4016*10^{-6}$**	**$0.7046*10^{-6}$**	**$0.3254*10^{-6}$**	**$0.8133*10^{-6}$**	**$0.4016*10^{-6}$**
PSNR(dB)	**113.0061**	**109.0285**	**112.0930**	**109.6514**	**113.0061**	**109.0285**	**112.0930**
SSIM	**0.9973**	**0.9962**	**0.9973**	**0.9970**	**0.9973**	**0.9962**	**0.9973**

Figure 5.1.2 till Figure 5.1.8 illustrate and validate that the direct inverse filter is satisfactory of restoring a motion blurred image. Consequently, the MSE, PSNR, and SSIM of direct inverse filter for motion blur is computed and tabulated in Table 5.1.

However, it is clear from Table 5.1 when the θ is equates 0°, the MSE showed the lowest value, while the SSIM is the highest value. Similarly, the results of 180° was same due to 180° is conjugated for 0°. In contrast, when the θ is equates 45°, the MSE showed the highest value, while the SSIM is the lowest value. Likewise, the results of 225° was same due to 225° is conjugated for 45°.

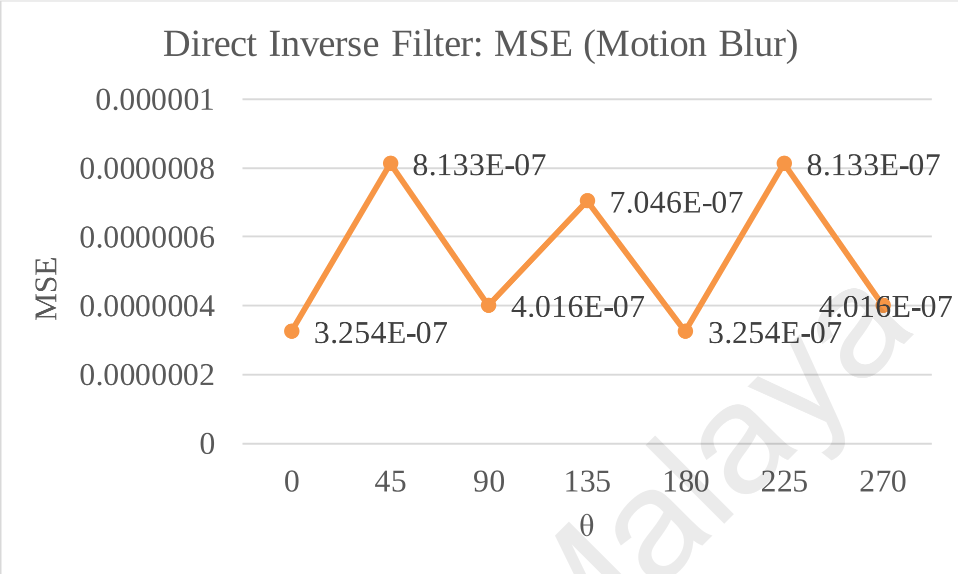

Figure 4.1.9 MSE of Direct Inverse Filter for Motion Blur

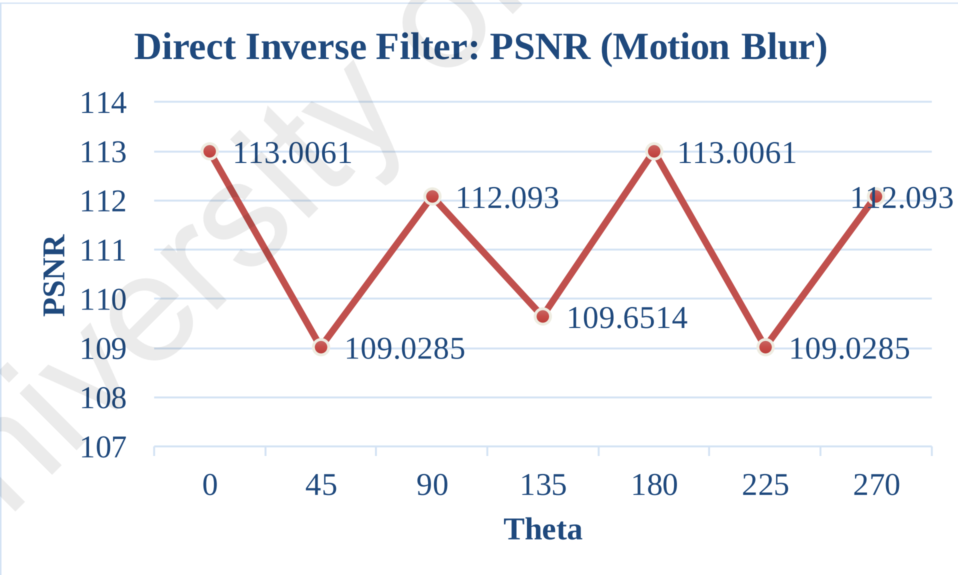

Figure 4.1.10 PSNR of Direct Inverse Filter for Motion Blur

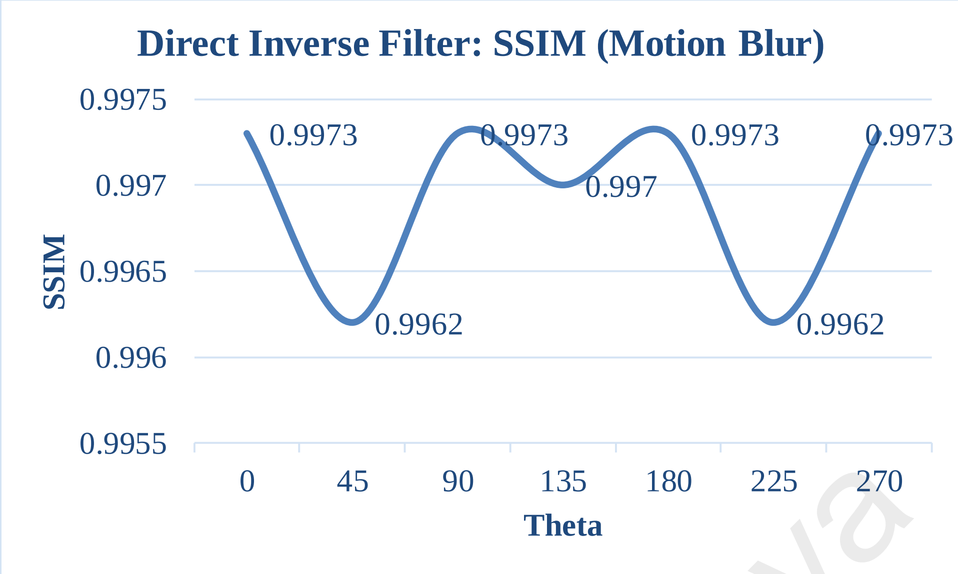

Figure 4.1.11 SSIM of Direct Inverse Filter for Motion Blur

4.2 Wiener Filter

Wiener filter is mathematically formulated as follows:

$$\hat{F}(u,v) = \left[\frac{|H(u,v)|^2}{\frac{S_N(u,v)}{S_F(u,v)} + |H(u,v)|^2} \times \frac{1}{H(u,v)}\right] \times G(u,v)$$

where $\hat{F}(u,v)$ is the optimal estimate of original image $F(u,v)$;$H(u,v)$ is the degradation/blurring/PSF/OTF function; $|H(u,v)|^2 = \overline{H(u,v)}H(u,v)$; $\overline{H(u,v)}$ is the complex conjugate of $H(u,v)$; $S_F(u,v) = |F(u,v)|^2$ is the power spectrum of the original image; $S_N(u,v) = |N(u,v)|^2$ is the power spectrum of the additive noise.

However, it is interesting to note that in the absence of noise, the noise to signal ratio, $S_N(u,v) \big/ S_F(u,v)$ is zero and the Wiener filter reduces to a direct inverse filter as follows:

$$\hat{F}(u,v) = \left[\frac{|H(u,v)|^2}{0 + |H(u,v)|^2} \times \frac{1}{H(u,v)}\right] \times G(u,v)$$

$$\hat{F}(u,v) = \frac{G(u,v)}{H(u,v)}$$

Figure 5.2.1 showed that the result of Wiener filter restored the motion blurred was better quality compared with the direct inverse filter. The computation of MSE, PSNR, and SSIM of Wiener filter was silently various to direct inverse filter. The MSE, PSNR and SSIM of the restored image are 0 and 121.9285 dB and 1 respectively, when θ and length are equate to 45o and 30 pixels respectively.

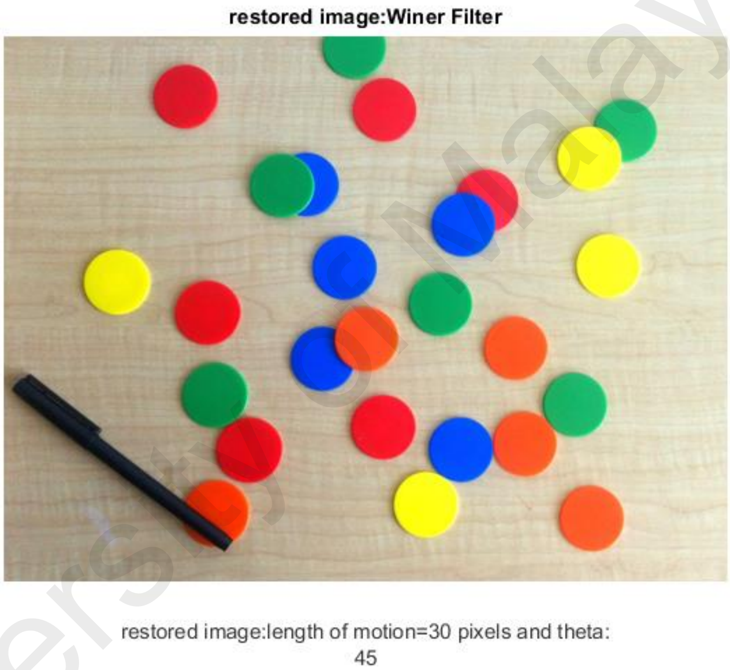

Figure 4.2.1 Image Restoration using Wiener Filter

Wiener filter is an enhanced image restoration technique that incorporates the blurring function into the image recovery process. The following is the MATLAB code of Wiener filter to restore motion blurred image.

```
sizeblurred=size(blurred); %size of degraded image
H=psf2otf(PSF,sizeblurred); %convert blurred function to spectral domain
%wiener Filter Formula
nom=conj(H).*1;
denom=(abs(H).^2);
denom=max(denom,sqrt(eps));
D=nom./denom;
restored=ifftn(D.*fftn(blurred));
```

Figure 5.2.2 till Figure 5.2.8. Presented the results of restored images of motion blurred.

Figure 4.2.2 Restored image using Wiener Filter at 0 degree

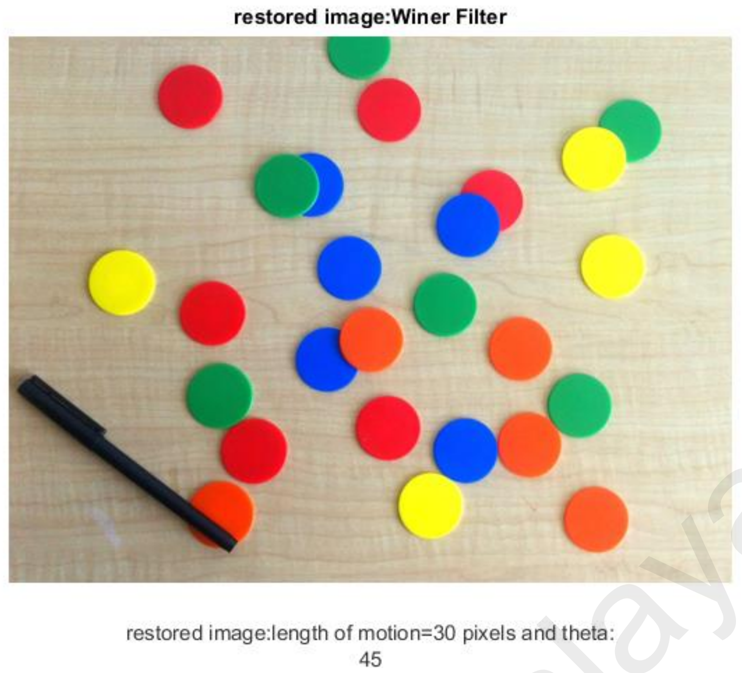

Figure 4.2.3 Restored image using Wiener Filter at 45 degree

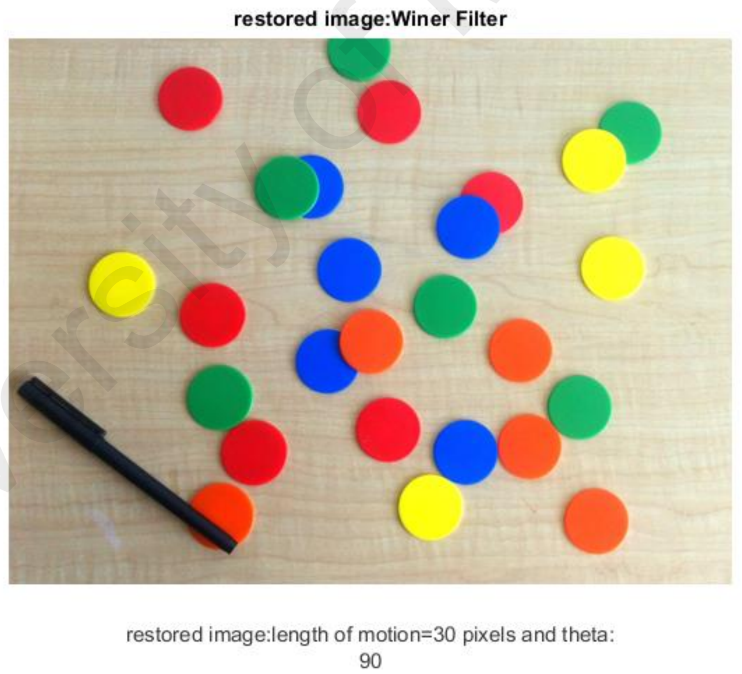

Figure 4.2.4 Restored image using Wiener Filter at 90 degree

Figure 4.2.5 Restored image using Wiener Filter at 135 degree

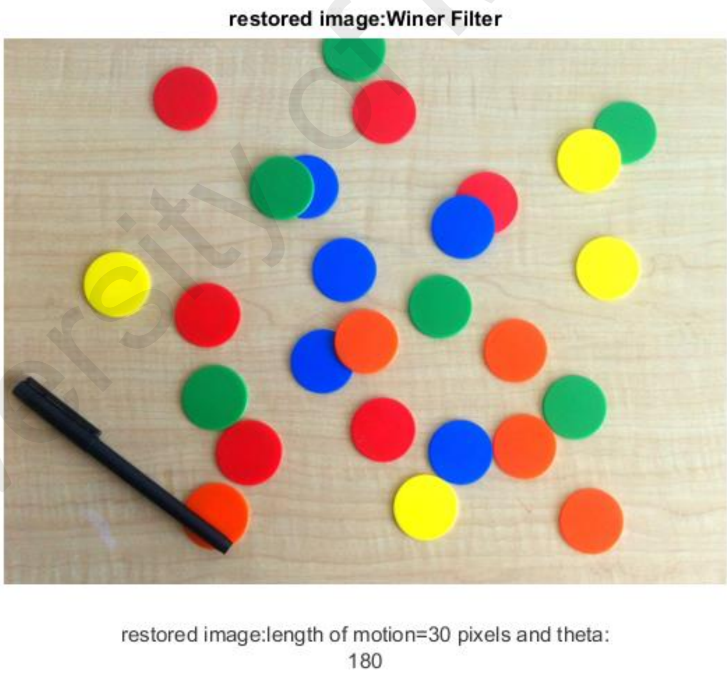

Figure 4.2.6 Restored image using Wiener Filter at 180 degree

Figure 4.2.7 Restored image using Wiener Filter at 225 degree

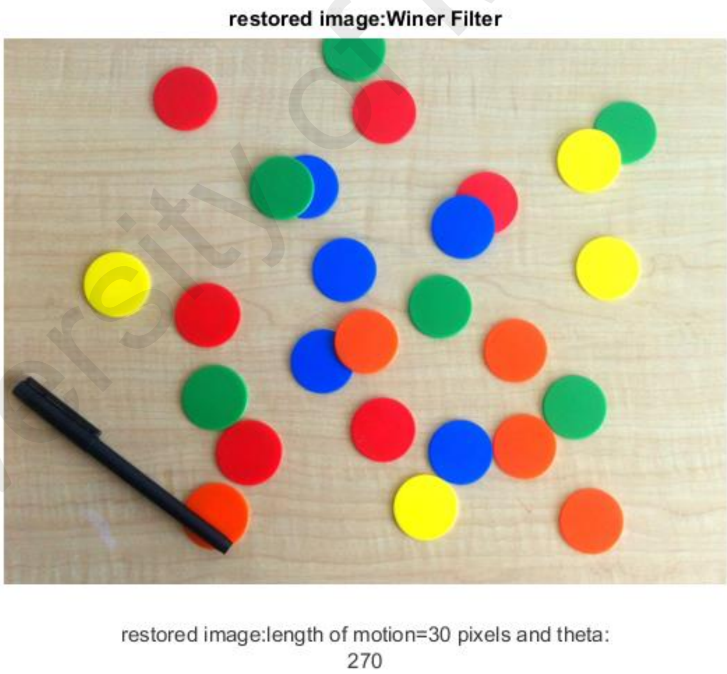

Figure 4.2.8 Restored image using Wiener Filter at 270 degree

The results of Wiener filter showed that the restored images are perfectly look like the original image. Consequently, the quantitative parameters, namely MSE, PSNR, and SSIM are computed and tabulated in Table 5.2 to compare and analyze the quality between the restored images and the original image. Generally, the cumulative squared errors between the restored images and original image are very minimal. Hence, the qualities of the restored images are quite good overall. However, it is clear from Table 5.2 when the θ is equates 0^{o}, the MSE showed the highest value, while the SSIM is the lowest value. Similarly, the results of 180o was same due to 180^{o} is conjugated for 0^{o}. In contrast, when the θ is equates 45^{o}, the MSE showed the lowest value, while the SSIM is the highest value. Likewise, the results of 225^{o} was same due to 225^{o} is conjugated for 45^{o}. Moreover, PSNR values are relatively high, and the luminance, contrast, as well as the structural similarities are quite close to the original image.

Wiener filter is indeed a more practical image restoration technique since it only requires knowledge of length and theta of blur, where can easily be estimated from the blurred image. Generally, the cumulative errors are particularly low, qualities are quite high, and pretty similar to the original image.

Table 4.2 MSE, PSNR and SSIM of Wiener Filter

Wiener Filter							
Theta	**0**	**45**	**90**	**135**	**180**	**225**	**270**
length	**30**	**30**	**30**	**30**	**30**	**30**	**30**
MSE	**$0.0125*10^{-3}$**	**0**	**$0.0099*10^{-3}$**	**$0.0008*10^{-3}$**	**$0.0125*10^{-3}$**	**0**	**$0.0099*10^{-3}$**
PSNR (dB)	**97.1616**	**121.9285**	**105.7600**	**119.0747**	**97.1616**	**121.9285**	**105.7600**
SSIM	**0.9975**	**1**	**0.9985**	**0.9998**	**0.9975**	**1**	**0.9985**

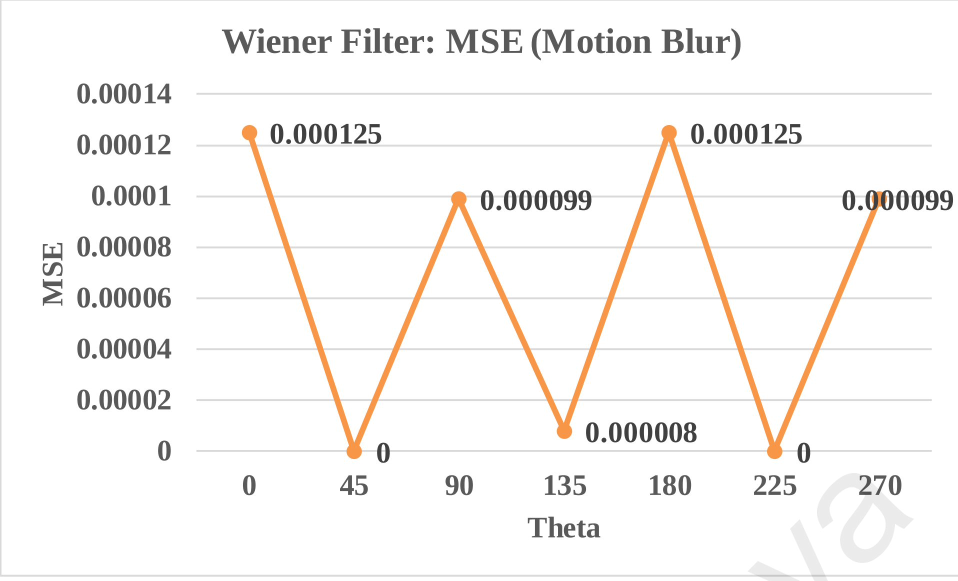

Figure 4.2.9 MSE of Wiener Filter for Motion Blur

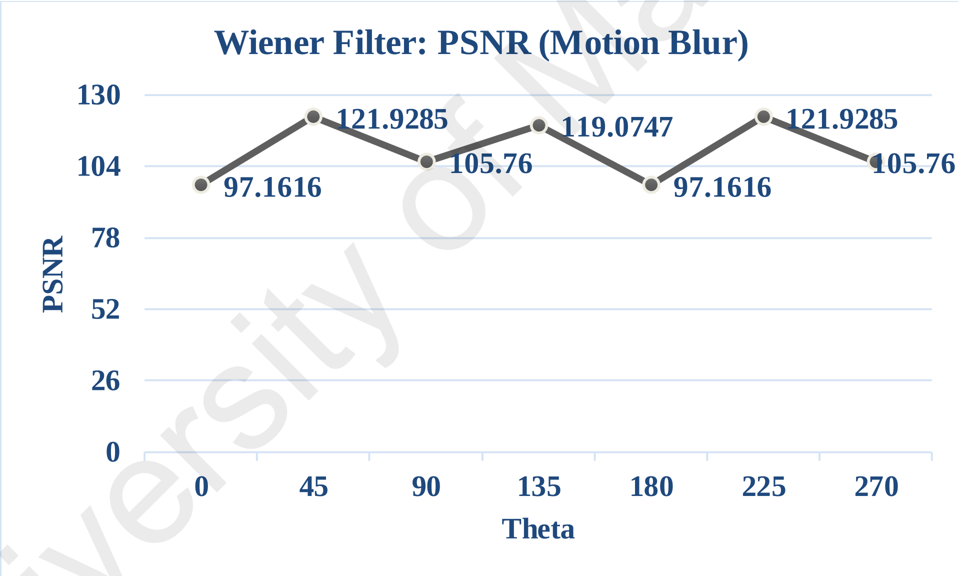

Figure 4.2.10 PSNR of Wiener Filter for Motion Blur

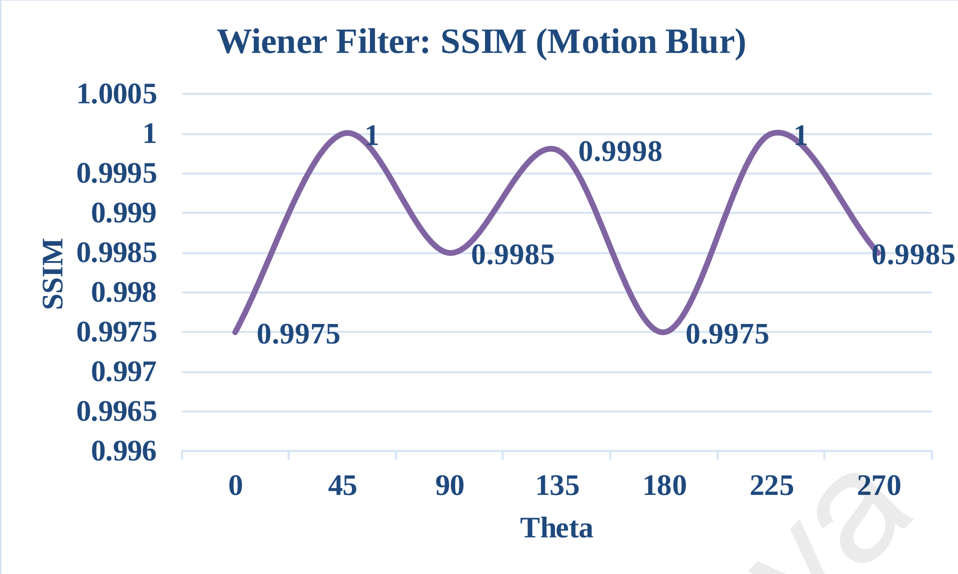

Figure 4.2.11 SSIM of Wiener Filter for Motion Blur

4.3 Constrained Least Squares (CLS) Filter

CLS filter is mathematically formulated as follows:

$$\hat{F}(u,v) = \left[\frac{|H(u,v)|^2}{|H(u,v)|^2 + \gamma|L(u,v)|^2} \times \frac{1}{H(u,v)}\right] \times G(u,v)$$

Where $\hat{F}(u,v) =$ the optimal estimate of the original image; $H(u,v) =$ the degradation/blurring/PSF/OTF function; $|H(u,v)|^2 = H^T(u,v)H(u,v)$; $H^T(u,v) =$ transpose of $H(u,v)$; $L(u,v)$ Fourier transform of Laplacian filter; and γ is an adjustable parameter to satisfy the constraint.

The only unknown in the CLS filter formulation is y however this unknown can be found iteratively if motion length and motion theta are known. In other words, the CLS filter requires only the length and theta of motion in the process of image restoration. The following is the MATLAB code of CLS filter to restore a motion blurred image:

```
sizeblurred=size(blurred);    %size of degraded image
    classblurred=class(blurred)    %class of degraded image
    sizePSF=size(PSF);    %size of blurred function
    classPSF=class(PSF);    %class of blurred function
    H=psf2otf(PSF,sizeblurred);  %convert blurred function to spectral domain
%CLS Filter Formula
nom=conj(H).* fftn(blurred);
    denom=(abs(H).^2+LAGRA*LAPLACIAN);
    denom=max(denom,sqrt(eps));
    restored = real (ifftn(nom./denom));
```

The restored images of motion blurred using CLS filter are illustrated and shown in Figure 5.3.1 till Figure 5.3.7.

4.3.1 Restored image using CLS Filter at 0 degree

4.3.2 Restored image using CLS Filter at 45 degree

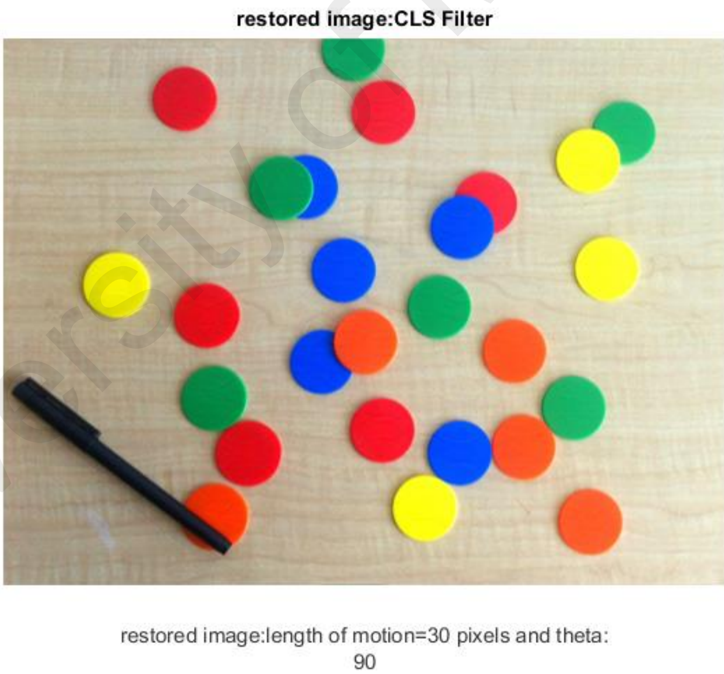

4.3.3 Restored image using CLS Filter at 90 degree

4.3.4 Restored image using CLS Filter at 135 degree

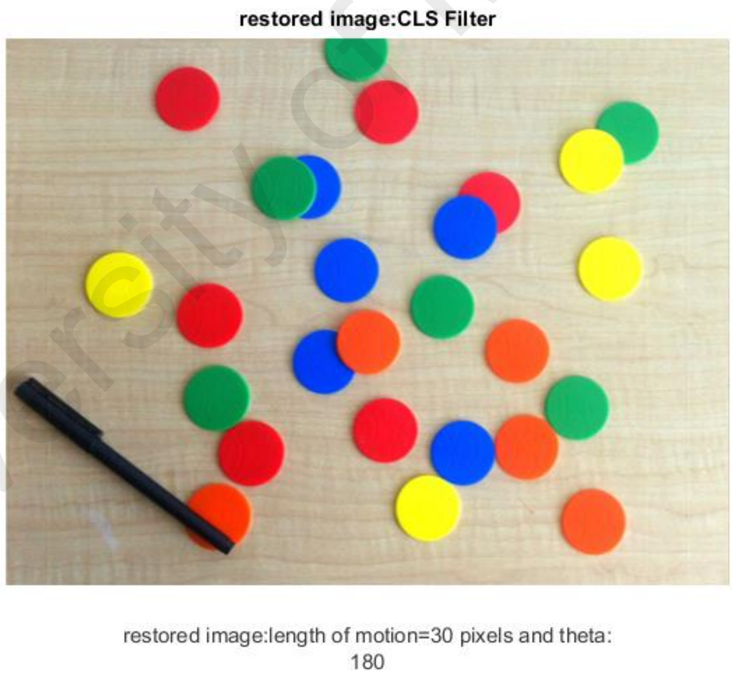

4.3.5 Restored image using CLS Filter at 180 degree

4.3.6 Restored image using CLS Filter at 225 degree

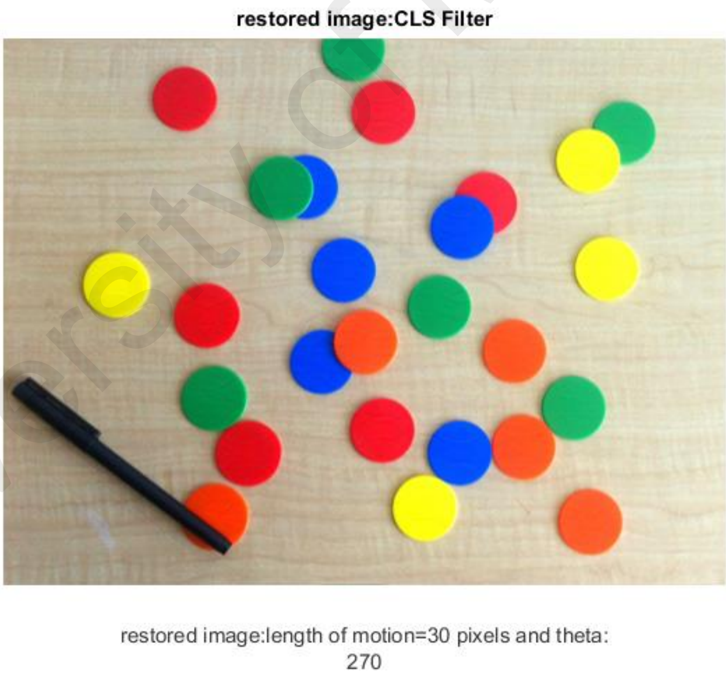

4.3.7 Restored image using CLS Filter at 270 degree

Qualitatively, the result quality of CLS showed that the restored images is different from the original. Consequently, the quantitative parameters, namely MSE, PNNR, and SSIM are computed and tabulated in Table 5.3. When the θ is equates 0^{o}, the cumulative error showed the lowest value, while the SSIM is the highest value. Likewise, the results of 180° was same because of 180° is conjugated for 0o. In contrast, when the θ is equates 45°, the MSE showed the highest value, while the SSIM is the lowest value. Similarly, the results of 225° was same due to 225° is conjugated for 45°.

Somewhat, CLS filter showed the lowest values compared to the other methods such as Direct Inverse filter and Wiener filter.

Table 4.3 MSE, PSNR and SSIM of CLS Filter

CLS Filter							
Theta	0	45	90	135	180	225	270
length	30	30	30	30	30	30	30
MSE	$0.6096*10^{-4}$	$0.7830*10^{-4}$	$0.7137*10^{-4}$	$0.7094*10^{-4}$	$0.6096*10^{-4}$	$0.7830*10^{-4}$	$0.7137*10^{-4}$
PSNR (dB)	90.2806	89.1930	89.5957	89.6220	90.2806	89.1930	89.5957
SSIM	0.9767	0.9697	0.9707	0.9718	0.9767	0.9697	0.9707

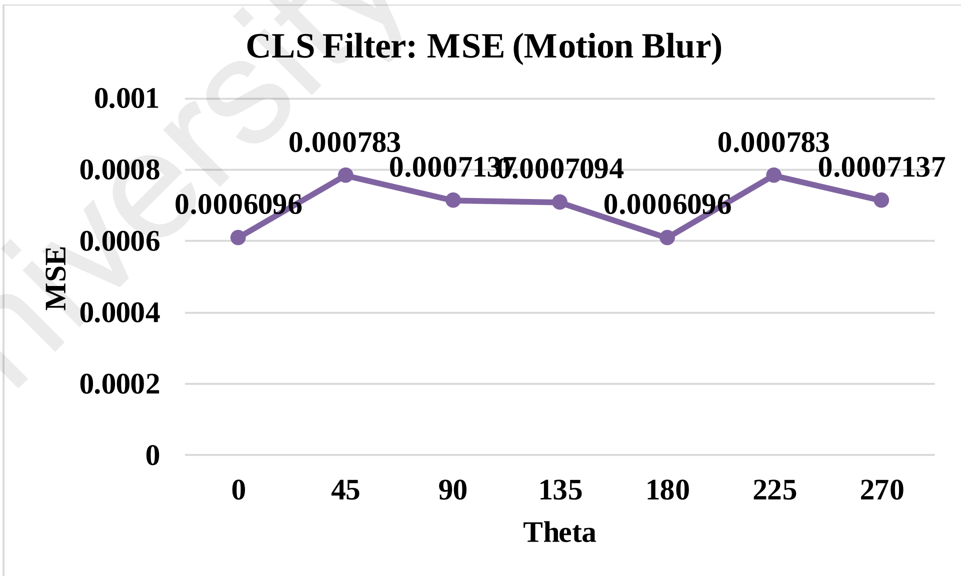

4.3.8 MSE of CLS Filter for Motion Blur

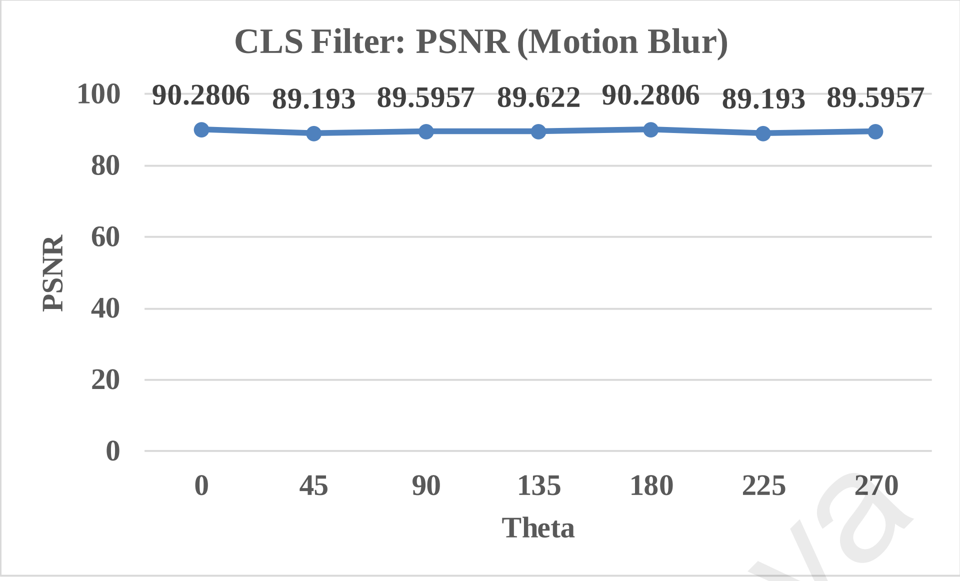

4.3.9 PSNR of CLS Filter for Motion Blur

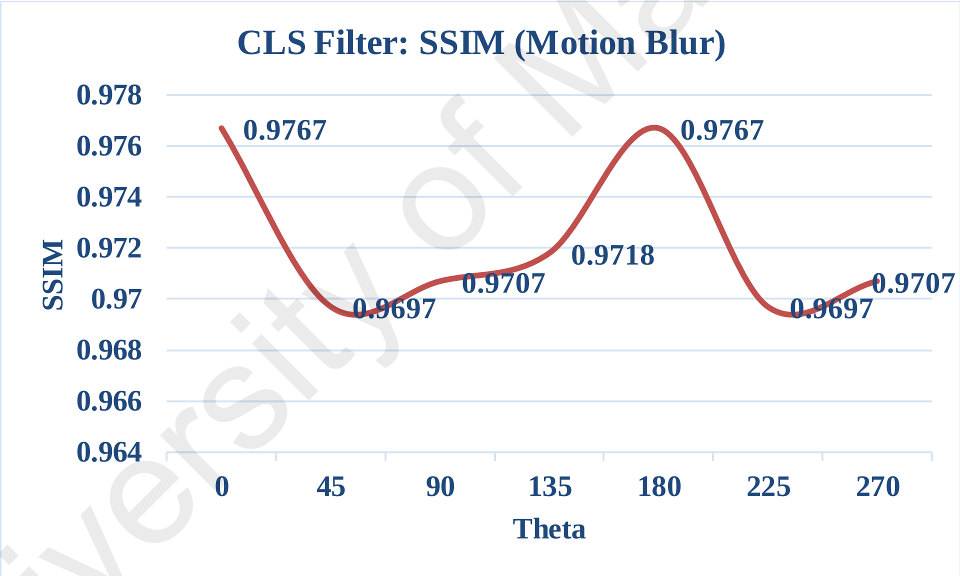

4.3.10 SSIM of CLS Filter for Motion Blur

4.4 Lucy Richardson (LR) Algorithm

LR algorithm is mathematically formulated as follows:

$$\hat{f}_{k+1}(x,y) = \hat{f}_k(x,y)\left[h(-x,-y) * \frac{g(x,y)}{h(x,y) * \hat{f}_k(x,y}\right]$$

Where $\hat{f}$ represents the estimate image, h is the point spread function, g is the degraded image, and * indicates convolution.

The restored images of motion blurred using LR filter are illustrated and shown in Figure 5.4.1 till Figure 5.4.7.

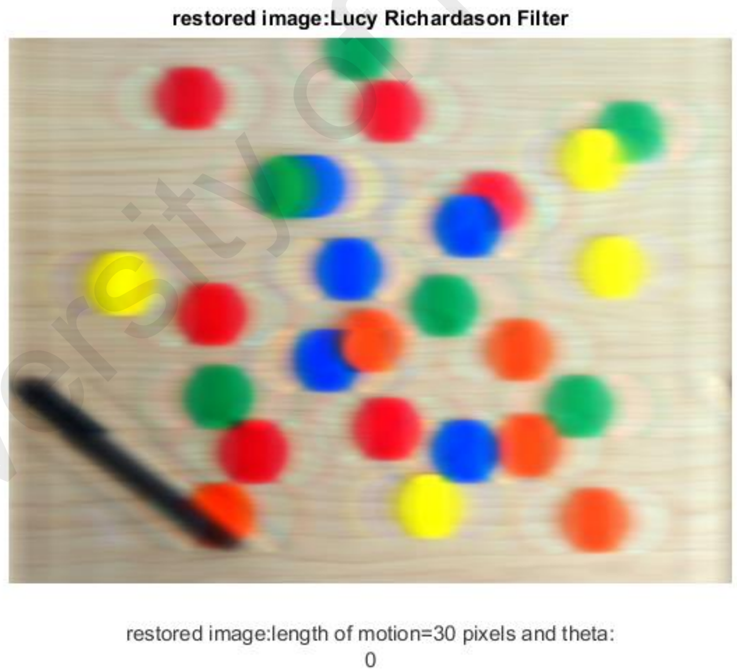

4.4.1 Restored image using LR Filter at 0 degree

4.4.2 Restored image using LR Filter at 45 degree

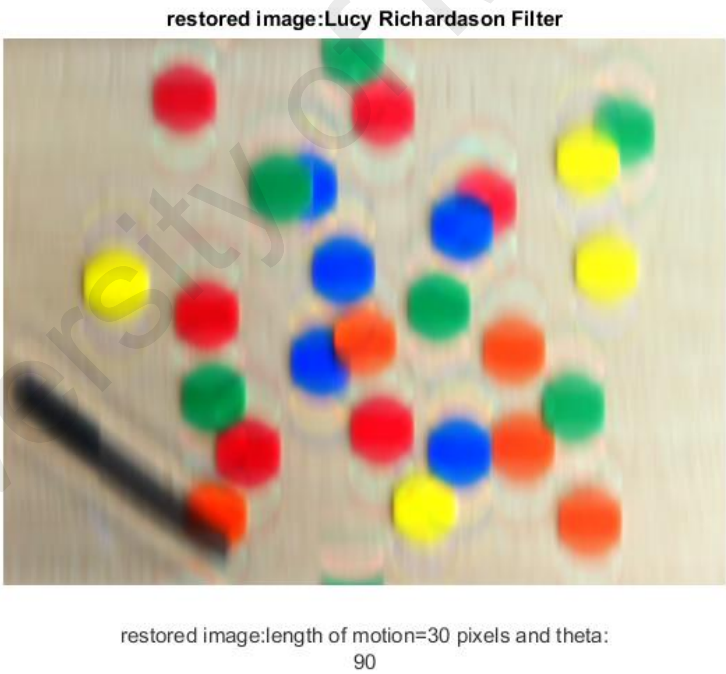

4.4.3 Restored image using LR Filter at 90 degree

4.4.4 Restored image using LR Filter at 135 degree

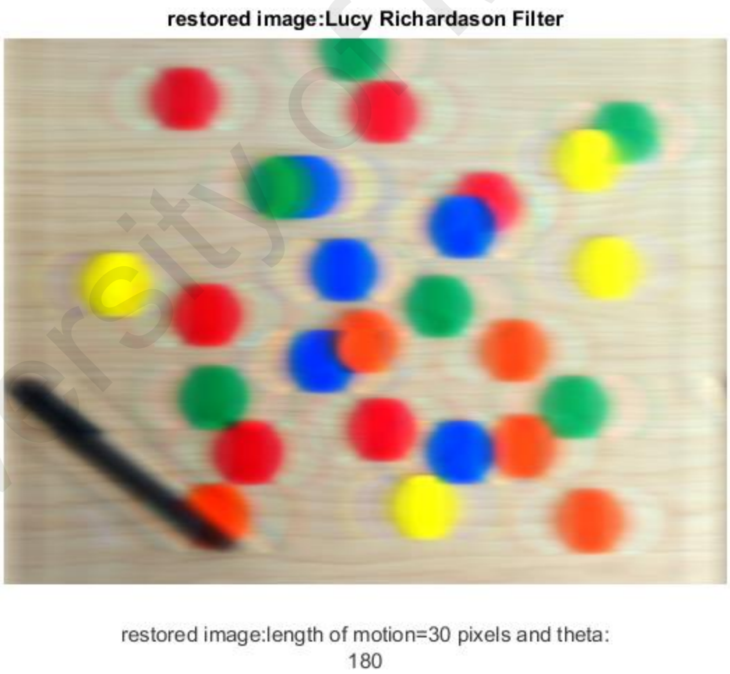

4.4.5 Restored image using LR Filter at 180 degree

4.4.6 Restored image using LR Filter at 225 degree

4.4.7 Restored image using LR Filter at 270 degree

Certainly, the restored images using LR algorithm are relatively poorest as compared with other methods. As a results, the image quality metrics, namely MSE, PSNR, and SSIM are computed to measure the quality of the restored images and presented in Table 5.4. Generally, the cumulative errors are quite small. Consequently, when the θ is equates

0^o, the MSE showed the highest value, while the SSIM is the highest value. Similarly, the results of 180^o was same due to 180^o is conjugated for 0^o. On the other hand, when the θ is equates 45o, the SSIM is the lowest value. Likewise, the results of 225^o was same because of 225^o is conjugated for 45^o.

Predictably, LR algorithm performs worse than Direct Inverse filter, Wiener filter and CLS filter.

Table 4.4 MSE, PSNR and SSIM of LR Filter

LR Filter							
Theta	**0**	**45**	**90**	**135**	**180**	**225**	**270**
length	**30**	**30**	**30**	**30**	**30**	**30**	**30**
MSE	**0.0025**	**0.0029**	**0.0026**	**0.0024**	**0.0025**	**0.0029**	**0.0026**
PSNR(dB)	**74.1286**	**73.4876**	**73.9759**	**74.3790**	**74.1286**	**73.4876**	**73.9759**
SSIM	**0.8455**	**0.7918**	**0.8088**	**0.8068**	**0.8455**	**0.7918**	**0.8088**

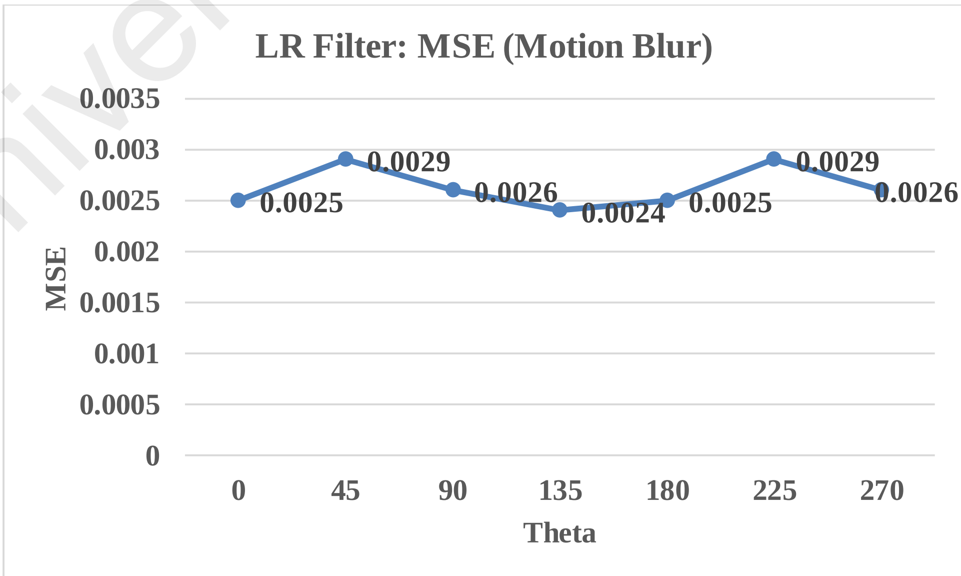

4.4.8 MSE of LR Filter for Motion Blur

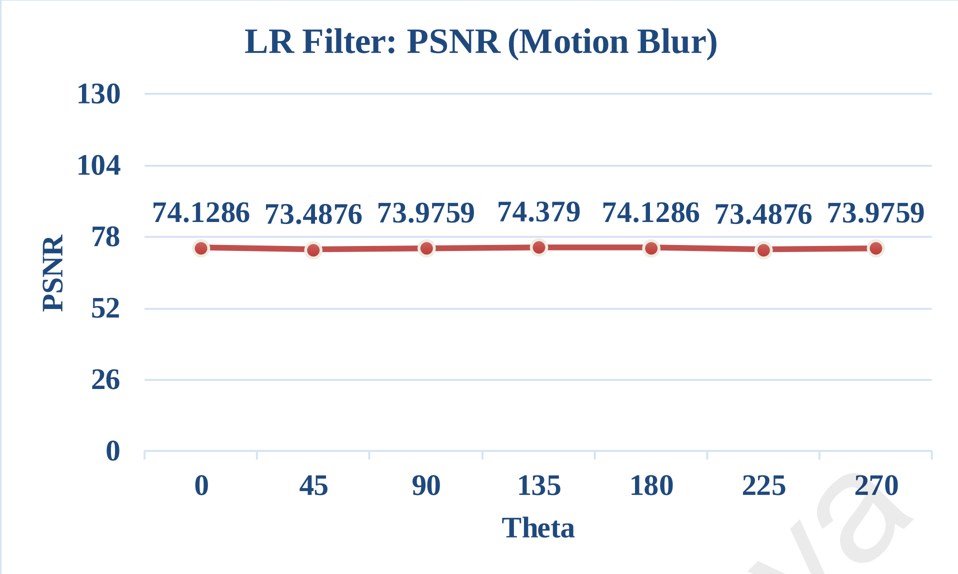

4.4.9 PSNR of LR Filter for Motion Blur

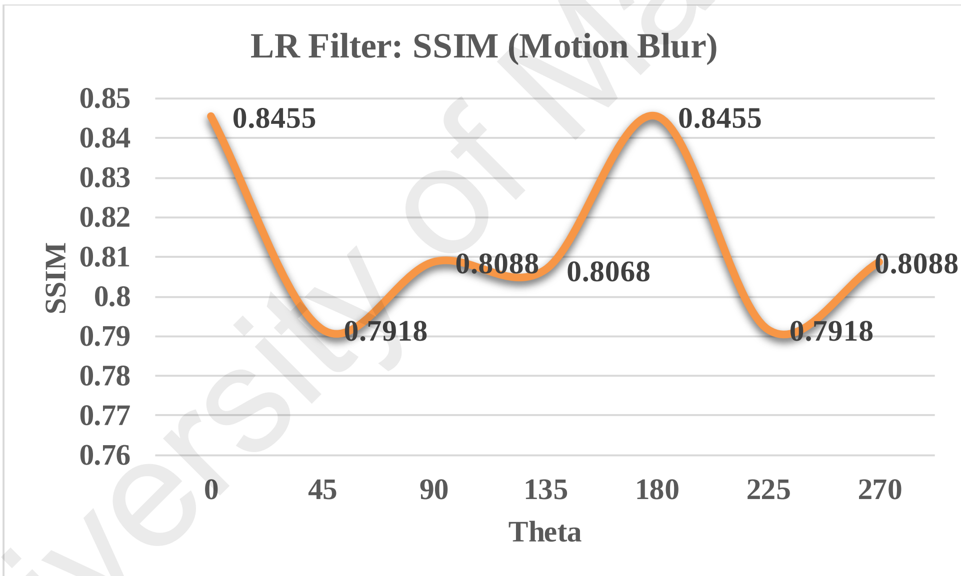

4.4.10 SSIM of LR Filter for Motion Blur

4.5 Comparison between Direct Inverse Filter, Wiener Filter, Constrained Least Squares Filter, and Lucy Richardson Filter

The results of four methods (i.e. Direct Inverse, Wiener, CLS, and LR filters) can be showed in Table 5.5, 5.6, and 5.7 for comparing the image quality metrics, namely MSE, PSNR, and SSIM. The image quality assessment of Wiener filter was achieved high performance in all aspects of the image compared with other methods like Direct Inverse filter, CLS filter, and LR filter. In contrast, LR filter is the poorest image restoration technique as it is vulnerable to blur and incapable of restoring motion blurred image. LR filter is designed for noise removal. The formulation of LR filter equation is for noise removal and that is a reason for not performing well for motion blur. Furthermore, CLS filter outperforms LR filter but loses out to Wiener filter and Direct Inverse filter.

The both CLS and LR filters do not require any knowledge about the original image in the process of image restoration. Hence, these techniques are indeed very handy in practice. However, the challenge of CLS filter lies in experimenting and determining the optimum Lagrange multiplier whereas the challenge of LR filter is in determining the optimum number of iterations.

It is interesting to observe that incorporation of the statistical properties of blurred and original image into formulation of Wiener filter makes it more attractive and suitable than Direct Inverse filter. Therefore, the challenge is to intelligently estimate the statistical properties of the original image until an acceptable restored image is obtained.

Observably, the performance of Wiener filter introduced high quality of image. Wiener filter minimize the mean square error between the estimate random process and the desired process. Wiener filter have been used with Fast Hartley Transform (FHT) to increase the speed of deblurring process. Moreover, it gave the preferable image restoration technique due to it not only performs slightly better but also requires shorter computational time and simply design than Direct Inverse filter. In addition, it is exploited the signal from begging, controlled yield error. Overall, the best-performing image restoration technique is Wiener filter, followed by Direct Inverse filter. CLS filter, and lastly LR filter.

Table 4.5 MSE of Direct Inverse Filter, Wiener Filter, CLS Filter and LR Filter

Mean Squared Error (MSE)							
Theta	**0**	**45**	**90**	**135**	**180**	**225**	**270**
length	**30**	**30**	**30**	**30**	**30**	**30**	**30**
Inverse	**0.000003254**	**0.000008133**	**0.000004016**	**0.000007046**	**0.000003254**	**0.000008133**	**0.000004016**
Wiener	**0.000125**	**0**	**0.000099**	**0.000008**	**0.000125**	**0**	**0.000099**
CLS	**0.0006096**	**0.0007830**	**0.0007137**	**0.0007094**	**0.0006096**	**0.0007830**	**0.0007137**
LR	**0.0025**	**0.0029**	**0.0026**	**0.0024**	**0.0025**	**0.0029**	**0.0026**

Table 4.6 PSNR of Direct Inverse Filter, Wiener Filter, CLS Filter and LR Filter

Peak Signal-to-Noise Ratio (PSNR)							
Theta	**0**	**45**	**90**	**135**	**180**	**225**	**270**
length	**30**	**30**	**30**	**30**	**30**	**30**	**30**
Inverse	**113.0061**	**109.0285**	**112.0930**	**109.6514**	**113.0061**	**109.0285**	**112.0930**
Wiener	**97.1616**	**121.9285**	**105.7600**	**119.0747**	**97.1616**	**121.9285**	**105.7600**
CLS	**90.2806**	**89.1930**	**89.5957**	**89.6220**	**90.2806**	**89.1930**	**89.5957**
LR	**74.1286**	**73.4876**	**73.9759**	**74.3790**	**74.1286**	**73.4876**	**73.9759**

Table 4.7 SSIM of Direct Inverse Filter, Wiener Filter, CLS Filter and LR Filter

Structural Similarity Index (SSIM)							
Theta	**0**	**45**	**90**	**135**	**180**	**225**	**270**
length	**30**	**30**	**30**	**30**	**30**	**30**	**30**
Inverse	**0.9973**	**0.9962**	**0.9973**	**0.9970**	**0.9973**	**0.9962**	**0.9973**
Wiener	**0.9975**	**1**	**0.9985**	**0.9998**	**0.9975**	**1**	**0.9985**
CLS	**0.9767**	**0.9697**	**0.9707**	**0.9718**	**0.9767**	**0.9697**	**0.9707**
LR	**0.8455**	**0.7918**	**0.8088**	**0.8068**	**0.8455**	**0.7918**	**0.8088**

CHAPTER 5: CONCLUSION & FUTURE DEVELOPMENT

5.1 Conclusion

In this study, four image restoration techniques were applied namely Wiener filter, Direct Inverse filter, Constrained Least Squares (CLS) filter, and Lucy Richardson algorithm. They were implemented, derived and analyzed based on a MATLAB software for reconstruct an original image that has intensively affected by motion blurred at fixed length (30 pixels) along with different angles (θ). At that time, image quality metrics, namely mean square error (MSE), peak signal-to-noise ratio (PSNR), and structural similarity index (SSIM) are operated to evaluate and measure the quality of the restored images. The results (Simulations and image quality metrics) revealed that Direct Inverse filter is reasonable for restoring a motion blurred image. CLS filter showed the low values compared to the other filter techniques as Direct Inverse filter and Wiener filter. In contrast, LR techniques presented poorest quality performs compared with other filter techniques, LR filter is designed for noise removal. Wanted to see how effective it can be for blur. The formulation of LR filter equation is for noise removal and that is a reason for not performing well for motion blur. Wiener filter is indeed a more practical image restoration technique since it only requires knowledge of length and theta of blur, where can easily be estimated from the blurred image. The results indicated that the performance of Wiener filter exhibited high quality of image compared with other filters. It presented the desirable image restoration technique because of it highly performs and also requires shorter computational time and simply design than other filters techniques. Wiener filter minimize the mean square error between the estimate random process and the desired process. Wiener filter have been used with Fast Hartley Transform (FHT) to increase the speed of deblurring process. Additionally, it exploited the signal from begging and controlled produce error. Wiener filter is the high-performing image restoration technique, followed by Direct Inverse, CLS, and, LR filters. Generally, the cumulative errors are particularly low, qualities are quite high, and pretty similar to the original image.

5.2 Future Development

This study used several image restoration techniques to overcome the degradation that caused by the motion blur. Thus, we need to develop one of the filters used in this study or create a new technique which may help to improve the restoration of the degraded image.

REFERENCES

C.Sasi varnan, A. J., Jaspreet Kaur, Divya Jyoti, Dr.D.S.Rao. (2011). Image quality assessment techniques pn spatial domain. *Int. J. Comput. Sci. Technol, 2*(3).

Dash, R., & Majhi, B. (2014). Motion blur parameters estimation for image restoration. *Optik-International Journal for Light and Electron Optics, 125*(5), 1634-1640.

Dosselmann, R., & Yang, X. D. (2008). *A formal assessment of the structural similarity index*: University of Regina. Department of Computer Science.

Eskicioglu, A. M., & Fisher, P. S. (1995). Image quality measures and their performance. *IEEE Transactions on communications, 43*(12), 2959-2965.

Furuya, H., Eda, S., & Shimamura, T. (2009). Image restoration via Wiener filtering in the frequency domain. *WSEAS transactions on signal processing, 5*(2), 63-73.

Gonzalez, R. C., Woods, R. E., & Eddins, S. L. (2010). *Digital Image Processing Using MATLAB®*: McGraw Hill Education.

Khare, C., & Nagwanshi, K. K. (2011). Implementation and analysis of image restoration techniques. *International Journal of Computer Trends and Technology-May to June*(2011).

Kudelka Jr, M. (2012). Image quality assessment. *Proceedings of Contributed Papers, WDS*, 94-99.

Li, C., & Bovik, A. C. (2010). Content-partitioned structural similarity index for image quality assessment. *Signal Processing: Image Communication, 25*(7), 517-526.

Mistry, D., & Banerjee, A. (2014). *Deblurred of Image with Wiener Filter in MATLAB.* Paper presented at the Journal of Emerging Technologies and Innovative Research.

Moghaddam, M. E., & Jamzad, M. (2006). Linear motion blur parameter estimation in noisy images using fuzzy sets and power spectrum. *EURASIP Journal on Advances in Signal Processing, 2007*(1), 068985.

Nisha, S. K. (2013). Image Quality Assessment Techniques *International Journal of Advanced Research in Computer Science and Software Engineering, 3*(7).

Petrou, M., & Petrou, C. (2010). *Image processing: the fundamentals*: John Wiley & Sons.

Sngulagi, P. (2015). Performance Analysis of Effective Image Restoration Techniques at Different Noises. *Indian J Sci Res, 11*(1), 009-016.

Stojanovic, I., Stanimirovic, P., & Miladinovic, M. (2012). Applying the algorithm of Lagrange multipliers in digital image restoration. *FACTA UNIVERSITATIS, Series Mathematics and Informatics, 27*(1), 41-54.

Thakur, M., & Datar, S. (2014). Image Restoration Based On Deconvolution by Richardson Lucy Algorithm. *algorithms*, *8*, 9.

Xavier, T. (2007). *Development of image restoration techniques.*

Yadav, M., & Omprakash, M. (2013). A Comparative Study for Deblurred Motion Blurred Images.

Yitzhaky, Y., Mor, I., Lantzman, A., & Kopeika, N. (1998). Direct method for restoration of motion-blurred images. *JOSA A*, *15*(6), 1512-1519.